Evaluation of SCIAMACHY Level-1 data versions using nadir ozone profile retrievals in the period 2003-2011

S. Shah[1], **O. N. E. Tuinder**[1], **J. C. A. van Peet**[1], **A. T. J. de Laat**[1], **and P. Stammes**[1]

[1]Royal Netherlands Meteorological Institute (KNMI), De Bilt, the Netherlands

Correspondence to: S. Shah (sweta.shah@aei.mpg.de) and P. Stammes (stammes@knmi.nl)

Abstract. ~~The depletion of the Antarctic ozone layer and its changing vertical distribution has been monitored closely by satellites in the past decades ever since the Antarctic "ozone hole" was discovered in the 1980's.~~ Ozone profile retrieval from nadir-viewing ~~satellites~~ satellite instruments operating in the ultraviolet-visible range requires accurate calibration of ~~level-1~~Level-1 (L1) radiance data. Here we study the effects of calibration on the derived ~~level-2~~Level-2 (L2) ozone profiles ~~and apply the retrieval to the Antarctic ozone hole region.~~

for three versions of SCIAMACHY L1 data: version 7 (v7), version 7 with m-factors (v7$_{\texttt{mfac}}$), and version 8 (v8). We retrieve nadir ozone profiles from the SCIAMACHY instrument that flew on-board Envisat using the Ozone ProfilE Retrieval Algorithm) (OPERA) developed at KNMI with a focus on ~~the~~ stratospheric ozone. We study and assess the quality of these profiles and compare retrieved ~~(~~L2 ~~)~~ products from L1 SCIAMACHY data versions ~~7 and 8 indicated as respectively (v7, v8) data~~ from the years 2003-2011 without further radiometric correction. From validation of the profiles against ozone sonde measurements, we find that the v8 performs better than v7 and v7$_{\texttt{mfac}}$ due to correction for the scan-angle dependency of the instrument's optical degradation.

~~The instrument spectral response function can still be improved for the L1 v8 data with a shift and squeeze. We find that the contribution from this improvement is a few percent residue reduction compared to reference solar irradiance spectra.~~ Validation for the years 2003 and 2009 with ozone sondes shows deviations of SCIAMACHY ozone profiles of $0.8\% - 15\%$ in the stratosphere and $2.5\% - 100\%$ in the troposphere, depending on the latitude and the L1 version used. Using L1 v8 for the years 2003-2011 leads to deviations of $\sim 1\% - 11\%$ in stratospheric ozone and $\sim 1\% - 45\%$ in tropospheric ozone. ~~Application of SCIAMACHY~~ The SCIAMACHY L1 v8 data ~~to the Antarctic ozone hole shows that most ozone is depleted in the latitude range from 70°S to 90°S. The minimum integrated ozone column consistently occurs around 15 September for the years 2003-2011. Furthermore~~from the ozone profiles for all ~~these years we observe that the value of the ozone column per layer reduces to almost zero at a pressure of 100~~can still be improved upon in the 265-330 ~~in the latitude range of 70°S to 90°S, as was found from other observations~~nm range used for ozone profile retrieval. The slit function can be improved with a spectral shift and squeeze, which leads to a few percent residue reduction compared to reference solar irradiance spectra. Furthermore, a bias correction in the reflectance for wavelengths below 300 nm appears to be necessary.

1 Introduction

Ozone (O_3) is one of the most important trace gases in our atmosphere. Stratospheric O_3 absorbs the dangerous solar ultra-violet (UV) radiation making it an important protector of life. A small amount of O_3 is found in the troposphere originating from stratospheric intrusions and from air pollution and photochemistry - this ozone is considered a health-risk.

Daily ozone monitoring using satellites dates back to the late 1970s with ~~instruments like~~ the Total Ozone Monitoring Spectrometer (TOMS, 1979) and Solar Backscatter Ultra Violet (SBUV) instruments, and since the mid-1990s also by the full UV/VIS ~~spectrum covering satellite instruments like the~~ spectral coverage instruments Global Ozone Monitoring Experiment (GOME, GOME-2) (e.g. Burrows et al., 1999; Munro et al., 2016), ~~Scanning~~ SCanning Imaging Absorption spectroMeter for Atmospheric ~~ChartograpHY~~ CHartographY (SCIAMACHY) (Bovensmann et al., 1999),

and Ozone Monitoring Instrument (OMI) (Levelt et al., 2006), to name a few. These successions of instruments allow us to compare long term global ozone layer behaviour and cross-check the quality of the measured data. A long-term Long-term monitoring of the ozone trend layer is primarily driven by global measurements of total ozone time series of such satellite data.

The vertical profile of ozone has traditionally been measured by in-situ electrochemical instruments attached to balloons(ozone sondes), so-called ozone sondes (Deshler et al., 2008), (Smit et al., 2007). Although ozone sondes provide the most an accurate method for ozone profile measurement, they are limited in the heights they can reach (< 35 km), and their geographical coverage is limited to approximately 300 stations worldwide that 70 stations worldwide (Staehelin, 2007). Ozone sondes provide weekly ozone sonde profiles, and very few stations with only few stations have a higher than weekly measurement frequency.

Satellite measurements provide an alternative means for obtaining globally global vertical ozone profiles. Ozone profile retrievals from nadir SBUV-type satellite instruments span for more than 40 years (Bhartia et al., 1996), (Bhartia et al., 2013). Successful retrievals are being performed from limb viewing instruments, like MLS, MIPAS, OSIRIS and OMPS-LP, as well as from occultation instruments like ACE-FTS, GOMOS and SAGE II. In general limb and occultation mode satellite instruments can well resolve the vertical distribution in stratospheric ozone. However, they are limited in their horizontal resolution, and they have no sensitivity to ozone in the middle and lower troposphere. An alternative approach is to use For that purpose satellite measurements in nadir mode by high-resolution spectrometers are required in the thermal IR, like IASI and TES TES (Worden et al., 2007) and IASI (Clerbaux et al., 2009), and in the UV/VIS, like GOME, GOME-2 (e.g. Cai et al., 2012; van Peet et al., 2014; Keppens et al., 2015; Miles et al., 2015). , OMI (e.g. Liu et al., 2010; Kroon et al., 2011), and SCIAMACHY.

The observation principle of nadir ozone profile retrieval in the UV/VIS is based on the strong spectral variation of the ozone absorption cross-section in the UV-visible wavelength range, combined with Rayleigh scattering. The key here is that the short UV wavelengths (265-300 nm) are backscattered from the upper part of the atmosphere whereas the longer UV wavelengths (300-330 nm) are mostly backscattered from the lower part of the atmosphere. This transition in the ozone cross-section between 265-330 nm is useful in retrieving its vertical profile. Nadir UV and visible spectra provide better a good horizontal resolution in ozone although their observations can only be carried out in daytime. In the thermal infra-red measurements can be done during both night and day.

SCIAMACHY had both limb and nadir mode capability. There have been several studies of ozone profiles using SCIAMACHY limb data (e.g. Brinksma et al., 2006; Mieruch et al., 2012; Hubert et al., 2017). Brinksma et al. (2006) found biases in ozone profile of stratosphere stratospheric ozone profiles of $< 10\%$. Also Mieruch et al. (2012) in their analysis of limb scatter ozone profiles from SCIAMACHY for 2002-2008 , Mieruch et al. (2012) found the stratospheric ozone have a bias found stratospheric ozone biases of $\sim 10\%$ against correlative data setsand this ; the bias increased up to 100% in the troposphere for the tropics. Similarly Hubert et al. (2017) in their more recent study of limb profiles find found that the SCIAMACHY ozone biases are about $\sim 10\%$ or more in the stratosphere with short-term variabilities of $\sim 10\%$. There has been very little published work on ozone profile retrieval from SCIAMACHY nadir mode, probably due to calibration issues.

In this study, we focus on nadir ozone profile retrieval from SCIAMACHY and the impact of L1 calibration improvements. We In this paper we compare and evaluate the three most recent versions of the SCIAMACHY L1 productdataset (described in Sect. 2) on the basis of retrieved . The comparison is based on the retrieval of the nadir ozone profiles from the SCIAMACHY UV reflectance spectra. , showing the impact of L1 calibration improvements. The three different L1 data versions used are: v7, v7$_{\mathrm{mfac}}$, and v8. The primary difference between them is the implementation of degradation correction. These data versions are described in Sect. 2. The result of this paper shows the improved quality of the latest L1 dataset version.

The results presented here highlight the need for further corrections of the L1 data. However, a detailed study of radiometric bias corrections in L1 data is beyond the scope of this paper. The focus of this study is to analyse stratospheric ozone and this study is done assess the quality of L1 data by analysing the retrieved ozone profiles. We do this for almost the entire mission length of 2003-2011 where validation is done globally and we perform validation for the latest L1 version available (v8). We will focus exclusively on the study of ozone in the stratospheric region (100–10), but we will briefly comment on the accuracies we get for tropospheric region (1000 – 100)version of the L1 data (v8). The OPERA retrieval algorithm is briefly reviewed in Sect. 2.2. In Sect. 3, the analysis of the slit function of the instrument is presented. Results on the Results of the ozone profiles, and the comparison between the level-1 datasets are shown in Sect. 4. 3. This is followed by comparison to sondes in Sect. 5 4 for the most recent dataset from the years 2003-2011spanning almost the entire mission. We apply the SCIAMACHY dataset in analysing the Antarctic ozone hole in Sect. 6. . We discuss the possible effects of L1 radiometric bias corrections and applying slit function corrections in Sect. 75, and finally conclude in Sect. 8. 6.

Table 1. SCIAMACHY Level 1 ~~(L1)~~ data characteristics in the range 265 - 330 nm used for ozone profile retrieval.

Wavelength range [nm]	Cluster number/Channel	Integration time [s]	spectral resolution [nm]
265-282	3/1	[0.125-1]	0.22
282-304	4/1	[0.125-1]	0.22
304-314	5/1	[0.125-1]	0.22
314-321	10/2	[0.125-1]	0.24
321-330	9/2	[0.125-1]	0.24

Integration time ranges from 0.125 s to 1 s depending on latitude.

2 Instrument, data and methods

SCanning Imaging Absorption spectroMeter for Atmospheric ChartograpHY (SCIAMACHY) is a space-borne spectrometer on board ESA's Environmental Satellite Envisat (Burrows et al., 1995; Bovensmann et al., 1999) ~~with both horizontal (limb) and vertical (nadir) mode viewing design covering the wavelength~~ that was launched in March 2002 and lasted until April 2012. The instrument measures the sunlight reflected by the Earth's atmosphere over a wide spectral range from 212 nm (UV) to 2386 nm (~~infrared, IR~~shortwave infrared, SWIR) spread over 8 channels. ~~Launched in March 2002, its mission lifetime spanned until 2012 and we have level-1 data (Lichtenberg et al., 2006) from the spectrometer from August 2002 until April 2012. In this paper we concern ourselves with the nadir data and in retrieving the vertical distribution of ozone using 265-330 UV-VIS continuous spectral data~~ SCIAMACHY can perform measurements in both nadir and limb viewing modes (Gottwald and Bovensmann, 2011). These modes usually alternate and the data collected are stored in blocks known as "states". Each nadir state is ~~an~~ essentially an observed area on the Earth's surface~~defined~~ , consisting of multiple ground-pixels.

The nadir viewing mode of the instrument corresponds to an Instantaneous Field of View (IFoV) of 0.045° (across track) × 1.8° (along track). The observed area is determined by the scan speed of the nadir mirror ~~across track directionand~~ in the across-track direction, the spacecraft speed in the ~~along track direction, the field of view (FoV)and the operation of the instrument~~along-track direction, and the integration time (IT). This gives typical ~~ground pixel sizes (or equivalently nadir states)~~ ground-pixel sizes of 240 km × 30 km ~~for an integration time (IT)~~ corresponding to an IT of 1.0 s and 60 km × 30 km for an IT of 0.25 s (Gottwald and Bovensmann, 2011). ~~Alternatively the nadir viewing corresponds to an instantaneous FoV (IFoV) of 0.045° (across track)~~ Typically, a nadir state is an area of 960 km× ≈ 500 km (across × ~~1.8°~~ (along track)~~. The IT also varies for clusters, the measurements should be combined before it is fed to the optimal estimation. The variation in IT between clusters can give rise to a spectral jump (discontinuity) where the last value of the spectral value in the preceeding cluster does not match the first value of the same in the following cluster. The wavelengths at which this occurs for Channels 1 and 2 were identified and blocked from our analysis (see Fig. 11 in Sect. 7).~~

~~The above specified wavelength range straddles~~ , consisting of 64 pixels containing the spectra to which ozone profile retrieval algorithm was applied. In order to perform radiometric calibration, SCIAMACHY also observes the Sun once per day.

The L1 data provided to users are generated from raw, uncalibrated Level-0 (L0) data by spectral and radiometric calibration ((Lichtenberg et al., 2006)). In this paper we retrieve the vertical distribution of the ozone using the 265-330 nm L1 data. This wavelength range spreads over Channels 1 and 2 of SCIAMACHY~~with an overlapbetween the two channels~~, with a partial overlap. We use wavelengths 265–314 nm from Channel 1 and 314–330 nm from Channel 2. The ~~extracted data from L1 are broken into states, which are groups of ground pixels. The~~ spectrum of each ~~ground pixel~~ channel is divided into spectral clusters which are groups of wavelengths ~~having their own~~ with a common integration time. These ~~are then organized into clustersof data instead of channels~~spectral clusters, and not the channels, are the organization structure of the data. The mapping of ~~clusters to wavelengths , the~~ wavelengths to clusters, the spectral resolution, and IT are listed in Table 1.

The ~~most important input for retrieving ozone profile are~~ main input quantity for retrieving the ozone profile is the Earth's reflectance ~~spectra (~~spectrum, derived from the L1 product~~). An example of these spectra are shown in Fig. 1. The observed~~ . In this paper the measured reflectance spectrum is defined as:

$$R_{\mathrm{meas}}(\lambda) = \frac{\pi I(\lambda)}{\mu_0 E(\lambda)} \frac{I(\lambda)}{E(\lambda)}, \qquad (1)$$

where ~~I, μ_0, and E are the radiance scattered and~~ λ is the wavelength, I is the top-of-atmosphere radiance reflected by the Earth's atmosphere ~~, the cosine of the solar zenith angle (θ_0), and~~ and surface, and E is the incident solar irradiance at ~~the top of the atmosphere~~ top-of-atmosphere perpendicular to the solar beam~~, respectively.~~

. We note that this definition of reflectance is also called the sun-normalized radiance. An example of a SCIAMACHY measured reflectance spectrum is shown in Fig. 1 for the spectral range used for the ozone profile retrieval.

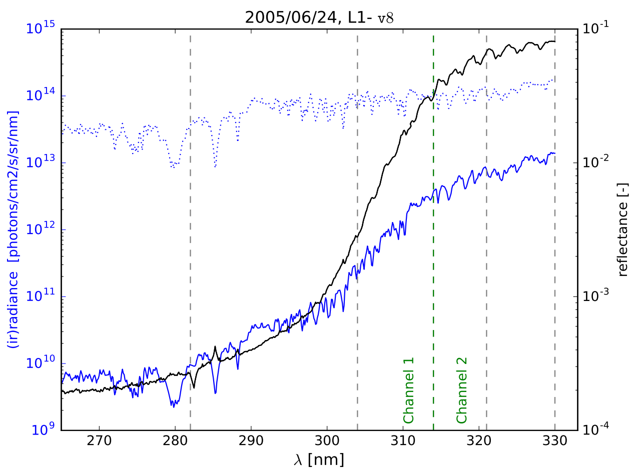

Figure 1. An example Example of the SCIAMACHY spectra of used for ozone profile retrieval: Earth radiance (solid blue line) and solar irradiance (dotted blue line) with the corresponding radiometric scale in [photons/cm2/s/sr/nm]indicated on the left side of the figure, and reflectance (solid black line) with the corresponding scale [unit-less]indicated on the right side of the figure. The vertical dashed line in green separates the two channels and the vertical grey lines separates separate the clusters as listed in Table 1.

2.1 Versions of level-1 (L1) Level-1 data

We make use of three different versions of The uncalibrated L0 data are processed into two sub-levels of L1products (described below) from the nadir spectral data : Levels 1b and present their differences using L2 products(ozone retrieval)1c. The SCIAMACHY specific calibrations applied to the L0 data are described in Slijkhuis et al. (2001). The two sublevels differ in the application of calibration steps: L1c data is processed by full calibration and contains geo-located, spectral radiance and irradiance products. Specifically the calibrated L1c data are reproduced produced using ESA's `SciaL1C` program of v3.2.6[1]. These versions we use in this paper are . We make use of three different versions of L1c (hereafter called L1) data products described below:

1. v7: L1 data products from SCIAMACHY are collocated spectra, radiometrically and spectrally calibrated radiances, including sun/moon occultation geometries. The version 7 (v7) specifically refers to This is SCIAMACHY L1 version 7.04 – W released in early 2012, where 'W' means the processing stage flag and 7.04 is the software version number used for converting raw level-1 to L0 into L1 product (SCIAMACHY L1 processor, IPP v7.04 – W) (?)data.

2. v7$_{\texttt{mfac}}$: This data set version is identical to the one described above, except here we use the degradation corrections correction factors, so-called "m-factors", that were provided independently as auxiliary data files[1]. Thus, the The data structure allows us to turn on and turn off to check the effects of the degradation corrections the degradation correction independent of other calibration corrections. Degradation correction is obtained by the so-called 'm-factors'. calibrations. The m-factors are determined by the monitoring of the light path which is given by the ratio of the measured spectrum of a constant source (Sun) to that obtained for the same optical path at a given time. This gives therefore an indication of the part of the the degradation of the optical path as the instrument ages. These m-factors are simple multiplication factors to the solar spectra spectrum after the absolute radiometric calibration (Gottwald and Bovensmann, 2011).

3. v8: The IPP This is version v8.02, which is the 2016 version of the SCIAMACHY L1 product. The main difference between this version with the ones and the one above is the implicit implementation of a standard degradation correction . The degradation in this version takes into account the with scan angle dependence of the nadir viewing geometry of the instrument with the optical path. We use the slit-function key data provided in v8 for the instrumental slit function retrieval (see Sect. 3). . Specifically the radiometric calibration uses a scan mirror model which takes into account the physical effect from of the contamination layers in on the mirror. The degradation using this model gives a scan angle dependence (Bramstedt, 2014).

2.2 OPERA retrieval algorithm

The Ozone Profile ProfilE Retrieval Algorithm (OPERA)has been , developed in KNMI (van Oss and Spurr, 2002; van der A et al., 2002). It , retrieves the vertical ozone profile using nadir satellite observations of back scattered UV sunlight scattered UV light from the atmosphereusing UV and visible wavelengths. The algorithm makes use of the laws of radiative transfer in computing radiative transfer computations of the top-of-atmosphere radiances given a number of the atmospheric scattering and absorption parameters. The ozone absorption cross-section decreases from 265 nm to 330 nm which allows us to retrieve the amount of ozone as a function of atmospheric height. The retrieval method is based on a forward model with a maximum

[1] https://earth.esa.int/documents/700255/708683/RMF_0140_SCI_NL__1 … fc23d1143d

[1] http://www.iup.uni-bremen.de/sciamachy/mfactors/

~~posteriori approach following Rodgers (2000). This amounts to obtaining the~~

In OPERA, the retrieval of ozone profiles uses the maximum a-posteriori approach Rodgers (2000). The state of the atmosphere ~~by using the radiative transfer model and inversion technique iteratively till the model atmosphere matches the measurement.~~ and the measurement are given by the vectors $\boldsymbol{x}$ and $\boldsymbol{y}$ respectively, and the two vectors are related by the forward model $\mathbf{F}$, according to $\boldsymbol{y} = \mathbf{F}(\boldsymbol{x})$. The solution is given by the following three equations:

$$\hat{\boldsymbol{x}} = \boldsymbol{x}_a + \mathbf{A}\left(\boldsymbol{x}_t - \boldsymbol{x}_a\right) \tag{2}$$

$$\hat{\mathbf{S}} = \left(\mathbf{I} - \mathbf{A}\right)\mathbf{S}_a \tag{3}$$

$$\mathbf{A} = \mathbf{S}_a\mathbf{K}^T\left(\mathbf{K}\mathbf{S}_a\mathbf{K}^T + \mathbf{S}_\epsilon\right)^{-1}\mathbf{K} \tag{4}$$

where $\hat{\boldsymbol{x}}$ is the retrieved state vector, $\boldsymbol{x}_a$ is the a priori, $\mathbf{A}$ is the averaging kernel, $\boldsymbol{x}_t$ is the "true" state of the atmosphere, $\hat{\mathbf{S}}$ is the retrieved covariance matrix, $\mathbf{I}$ is the identity matrix, $\mathbf{S}_a$ is the a priori covariance matrix, $\mathbf{K}$ is the weighting function matrix or Jacobian (which gives the sensitivity of the forward model to the state vector) and $\mathbf{S}_\epsilon$ is the measurement covariance matrix.

The matrices $\mathbf{A}$ and $\hat{\mathbf{S}}$ provide valuable information on the retrieval. The sum of the diagonal elements of $\mathbf{A}$ (i.e. the trace) is called the Degrees of Freedom for Signal (DFS). The higher the DFS, the more the retrieval has learned from the measurement. On the other hand, with a low DFS most information in the retrieval is coming from the a-priori. The total DFS gives the number of independent pieces of information present in the retrieval. The rows of $\mathbf{A}$ are called the smoothing functions, since they give an indication of how $\boldsymbol{x}_t$ is smoothed out over the layers of the retrieval. The diagonal elements of the covariance matrix give the variance at the corresponding altitude, while the off-diagonal elements are related to the correlation between the layers in the retrieval. For a comprehensive algorithm overview and retrieval configuration, along with ~~a description of the evaluation of the algorithm and the application~~ application of the algorithm to GOME-2 data, we refer to (Mijling et al., 2010; van Peet et al., 2014). ~~The~~

The OPERA configuration chosen for ~~all the retrievals are tabulated~~ application to SCIAMACHY data is given in Table 2. The ~~retrieval grid or the vertical resolution of the nadir profile in OPERA can be~~ ozone profile retrieval grid is chosen according to the Nyquist criterion. For SCIAMACHY data we find that setting the ~~vertical grid to 32~~ retrieval grid to 31 layers or more gives the same value for the ~~degrees-of-freedom (DFS). DFS (used in the Results section below) is a number related to~~ DFS. Following (van Peet et al., 2014), we have used the ~~averaging kernels of the instrument or the sensitivity of the instrument with vertical height.~~ (McPeters et al., 2007) a-priori ozone profiles, because it is a recent climatology (includes ozone depletion) and unlike other climatologies it does not require additional parameters like total ozone. Since the (McPeters et al., 2007) a-priori profiles do not contain covariance matrices, these are assumed to have an exponential decrease in pressure and are scaled with a-priori errors (for details see van Peet et al. (2014)). OPERA can also use the (Fortuin and Kelder, 1998) climatology. The reflectance measurement errors are provided in the SCIAMACHY L1 data; a systematic relative error in the measured reflectance ("noise floor") of 0.015 is added to the measurement errors. The noise-floor is assumed the same for all L1 data.

~~Relative residuals of daily SCIAMACHY L1 v8 solar spectra for Channels 1 and 2. G, O, D, S are Gain, Offset, Displacement/Shift and Squeeze respectively, where M is SCIAMACHY Measurement and S is Simulation (or modified model reference, see text). For visibility the residuals for ~ 300 spectra are shown spread throughout the mission length from August 2002 to April 2012.~~

~~Temporal evolution of the slit function parameters shown for Channels 1 (top row) and 2 (bottom row). This is shown for the entire mission for 3466 days where Year 0 means 2002 and Year 8 means 2010.~~

In practice, the ~~measurement (reflectance spectrum)~~ measured reflectance spectrum $R_{\text{meas}}(\lambda)$ ~~in~~ (see Eq. 1) is prepared in the beginning of the OPERA algorithm, which is then passed to the ~~Forward~~ forward model. This model contains vertical atmospheric profiles, ~~temperature, a priori~~ like temperature and a-priori ozone profile, geolocation, cloud data, and surface characteristics. The forward model ~~is used to compute simulated radiance at the~~ computes sun-normalized radiances at top-of-atmosphere at wavelengths determined from the measured instrumental spectral data. ~~This is further used to generate reflectances by using convolved simulated solar irradiance spectrum~~After multiplication with a high-resolution solar irradiance reference spectrum and convolution of simulated radiances and irradiances with the instrumental slit function, the simulated reflectance spectrum $R_{\text{sim}}(\lambda)$ is obtained. The inversion step that follows is based on the Optimal Estimation method requiring measurement, simulation and measurement ~~uncertainties~~ errors in vector/matrix forms. An inversion using derivatives of simulated reflectances with respect to the desired parameter to be solved is carried out until convergence is reached or until the maximum number of iterations is reached. For a comprehensive description of the ~~flow~~ implementation, configuration and the model parameters of the algorithm we refer to the OPERA manual (Tuinder et al., 2014).

3 ~~Instrumental Slit Function calibration of the Solar spectral measurement~~

The accuracy of the retrieved geophysical product is primarily driven by the quality of the measured spectra, $R_{\rm meas}(\lambda)$ (Eq. 1), and its spectral and radiometric calibration. The most important SCIAMACHY specific calibration applied to the level-0 (raw data) is described in Slijkhuis et al. (2001). One of the spectral calibrations done often to assess the degradation of the instrument in-flight is a fit of the instrument slit function (SF). It describes the behaviour of the projection of the incoming light onto the detector pixels. These were measured for SCIAMACHY on ground before launch (2002) and they are provided as L1 key data for the instrument that measures the solar spectra, $E(\lambda)$ (Eq. 1). The slit function of the instrument has different functional forms depending on which channel they belong to. For Channels 1-2 (relevant for our ozone retrieval) they are described by a single hyperbolic function:

$$\mathcal{S}(\lambda) = \frac{1}{a^2 + \lambda^2}.$$

The L1 key data provides the full width half maximum (FWHM) measured on ground which is related to the a parameter in the equation above. This parameter can be solved in terms of the FWHM by using the fact that at the central point (λ_0): $S(\lambda_0) = 1/a^2$. Thus, $a = \frac{\rm FWHM}{2}^2$. At each given solar spectrum wavelength, λ_i, this functional shape is numerically computed between -1,1 centred at λ_i. This shape can be manipulated with the SF parameters: additive constant (Offset, O), multiplication factor (Gain, G), Displacement of the peak along wavelength (Shift, D) and expansion and contraction of the spectral peak (Squeeze, S). The high resolution solar spectrum (Simulation) from Dobber et al. (2008) is modified with these four parameters to best match the SCIAMACHY measured solar intensity (Measurement, $E(\lambda)$). First spectral parameters, shift, D and squeeze, S are applied to Eq. 5:

$$\mathcal{S}'_{\rm SD}(\lambda) = \mathcal{S}(\lambda[1 - S(\lambda)] + D(\lambda)),$$

followed by radiometric parameters, gain G and offset O:

$$\mathcal{S}'_{\rm GOSD}(\lambda) = [\mathcal{S}'_{\rm SD}(\lambda)G(\lambda)] + O(\lambda),$$

The unit of Shift, D is and of Offset, O, Gain, G and Squeeze, S are numeric factors and all four parameters depend on wavelength. The parameters FWHM and λ_0 at each wavelength taken from the v8 L1 key data were identical for all the solar spectra throughout the mission. These values are given at certain wavelengths spread throughout Channels 1 and 2 and were interpolated for the wavelengths in between. An Optimal Estimation (OE) algorithm is used to solve for the best fit parameter values using the solar measurements after the launch. The retrieved values at the solar spectrum wavelengths are then also applied to the Earth radiance spectra $I(\lambda)$ (Eq. 1) interpolated at the solar spectrum wavelengths.

Thus for each solar spectrum wavelength the parameter values are used in the retrieval algorithm. These best fit values are computed using the slit function model with the above mentioned four ways of manipulation. The manipulations are that each spectral peak of the model spectrum (reference) can be transformed with: Offset, Gain, Shift, and Squeeze. Each of these spectral manipulations can be modelled as a polynomial of order n for each slit function of the instrument at the desired channels. The OE was run using this model from which the best values of the Offset, Gain, Shift, Squeezeas a function of wavelength of Channels 1 and 2 are retrieved. The best fit value is checked by evaluating the relative difference between the Solar Irradiance Measurement and Simulation which is the relative residual. The relative residuals for the best fit $\{O, G, D, S\}$ are shown in Fig. 9. Each curve is a residual for one solar spectrum where the blue line is achieved by using only gain and offset in the model and the red line is achieved by including the shift and/or squeeze.

We find that in Channel 1, the wavelength range 265-308 is the optimal range for obtaining smallest residuals. However because the ozone profile retrieval algorithm requires data from 260 , we do the optimal estimation from 260-308 . The higher wavelength values around 314 in Channel 1 are known to have had calibration problems and therefore we use them only until 308where the slit function retrievals are still well behaved. The irradiances at 308-314 in Channel 1 failed to match the model spectrum. We ran the optimal estimation on all solar measurements of the SCIAMACHY mission for each day which amounted to 3463 solar spectra. We convolved all spectra with {Offset, Gain, Shift, Squeeze} of polynomial orders of = $\{2, 15, 2, -\}$ and found that the cost function for the majority of cases reaches less than 1 (as expected) within 10 loops of retrieval in the Optimal Estimation routine. We find that using Shift in range 265-308 in Channel 1 reduces the residuals significantly looking at the left-panel in Fig. 9.

The residuals in Channel 2 are larger throughout. Dividing the relevant range of 308-330 into smaller ranges to get smaller residuals did not reduce the residuals any further. For the optimal wavelength divisions, we found the least residuals given by the polynomial orders of the set of {Offset, Gain, Shift, Squeeze} = $\{1, 4, 1, 2\}$. In Channel 2, shown in the right panel, we find that using Shift, Squeezein the range 308-330 reduces the relative residuals significantly. The relative errors of the observation in the wavelength range which we will use for ozone retrieval, 265-330 , are in the order of 10^{-5}. The relative residuals are in the order of a few percent. So we expect an error of a few percent to propagate into the ozone retrieval despite more accurate solar irradiances. There are anomalies in the residuals at around 279 , 280 and 285 . These are due to the strong and lines from the solar spectra and will not be used for ozone retrieval as indicated in Table 2.

~~Figure 10 shows the temporal dependence of all the slit function parameters for Channel 1 (top row) and Channel 2 (bottom row) as density plots where the value for each wavelength and each day of the year is shown. The ranges of the values are to the right to each figure. The seasonal dependence of solar radiation is observed as expected in the parameter Gain (first column of the figure) for both channels. The other parameters do not show any seasonal dependence over the mission time.~~

~~Top-left: Measured reflectance spectra for the year 2003. The spectra are an average over all the pixels in the range of the geolocations around the sonde stations within a narrow tropic latitude bands from 10°N to 10°S. Top-right: Corresponding retrieved ozone profiles (in Dobson Units per layer) with different colours representing various versions of L1 SCIAMACHY data used (described in Section 2). The versions 7 with and without the degradation corrections almost overlap (blue and green lines) whereas version 8 with improved degradation correction has a visible difference in the ozone profile. Bottom rows are for the year 2009. Note the remarkable difference between v7 and later versions with degradation corrections. Here the later two versions almost overlap compared to the case where no degradation is taken into account showing the significant difference in L1 data between the three versions when degradation of the instrument is not taken into account. The number of pixels in each data set with corresponding uncertainties are listed in Table 3.~~

As mentioned above, the averaging kernel (AK) of a retrieval represents the measurement sensitivity with respect to the true state of the atmosphere Rodgers (2000). In Fig. 2 we show an example of the AK for an individual OPERA ozone profile retrieval for a SCIAMACHY state on 2004/01/07. The AK rows represent the smoothing of the true profile as a function of the ozone retrieval layers. These smoothing functions should peak at the corresponding retrieval level and the half-width is a measure for the vertical resolution of the retrieval at that altitude. For an ideal retrieval, the curve of each row will peak at the nominal layer height with a spread that gives the vertical resolution of the retrieval. It is clear from Fig. 2 that information on the ozone amount in a certain layer is also coming from other heights.

3 Results: ~~ozone~~ Ozone profiles for different L1 versions

We ~~perform~~ have performed OPERA retrievals on SCIAMACHY nadir data for almost the entire mission length (2003-2011) ~~on geolocations close in space and time to ozone sondes. Here we use profiles in the vicinity of the sondes as a guidance for a general comparison between the three datasets used. Thus the results presented in this section are for pixels (states) with global coverage for all the months of the years2003 to 2011. In Sect. 4.1 we~~ for a narrow range of latitude band from 10° N to 10° S. We have excluded the years 2002 (beginning of the mission) and 2012 (end of the mission) since there are only few months of data in those years. We show the comparison ~~of the validation results for~~ between the L2 products retrieved from the three different ~~dataset versions for selected years. This is followed by validation results using v8 dataset for all the years, 2003-2011. The main focus of this study is to analyse SCIAMACHY nadir ozone profiles in the stratosphere, using~~ L1 dataset versions, v7, $\texttt{v7}_{\texttt{mfac}}$, and v8 ~~L1 data thus verifying their usefulness for ozone profile studies. With a nadir-viewing instrument it is very hard to retrieve an accurate ozone profile in the troposphere which ranges in pressure height from $\sim 1000 - 100$. The lower-middle stratosphere ranges from $\sim 100 - 10$ which is the main focus of this paper as motivated in Sect. 1 above. Thus in the subsections below we will present a discussion of the quality of the SCIAMACHY nadir O_3 profiles in the lower-middle stratosphere and compare it to the results from other existing studies.~~

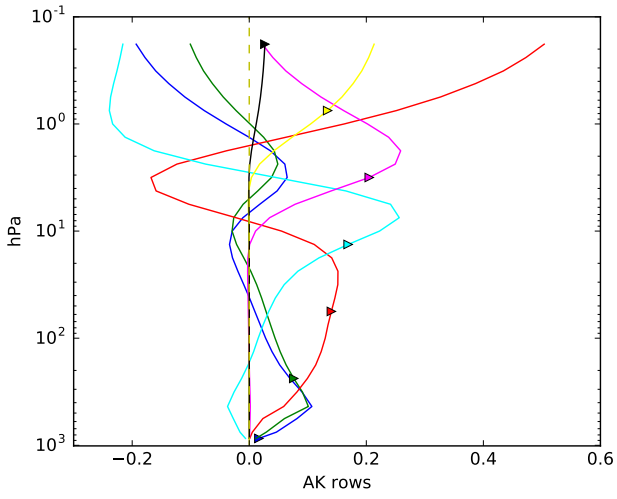

Figure 2. Example of the averaging kernel shape for a subset of seven layers from a 31-layer SCIAMACHY ozone profile retrieval. The triangles are the nominal altitudes of the retrieval layers. This subset of seven retrieval layers was selected uniformly ranging from top to bottom for clarity.

3.1 ~~Comparison of the ozone profiles using datasets v7, $\texttt{v7}_{\texttt{mfac}}$, and v8~~

~~We make~~ (described in Sect. 2.1) for the years 2003 and 2009 below. We have made a direct comparison of nadir ozone profiles and their corresponding reflectance spectra (with converged retrievals) between the different dataset versions. ~~We show the comparisons~~ The comparisons are performed for the years 2003 and 2009 to show how the ~~differences in the~~ reflectance measurements (and therefore the profiles de-

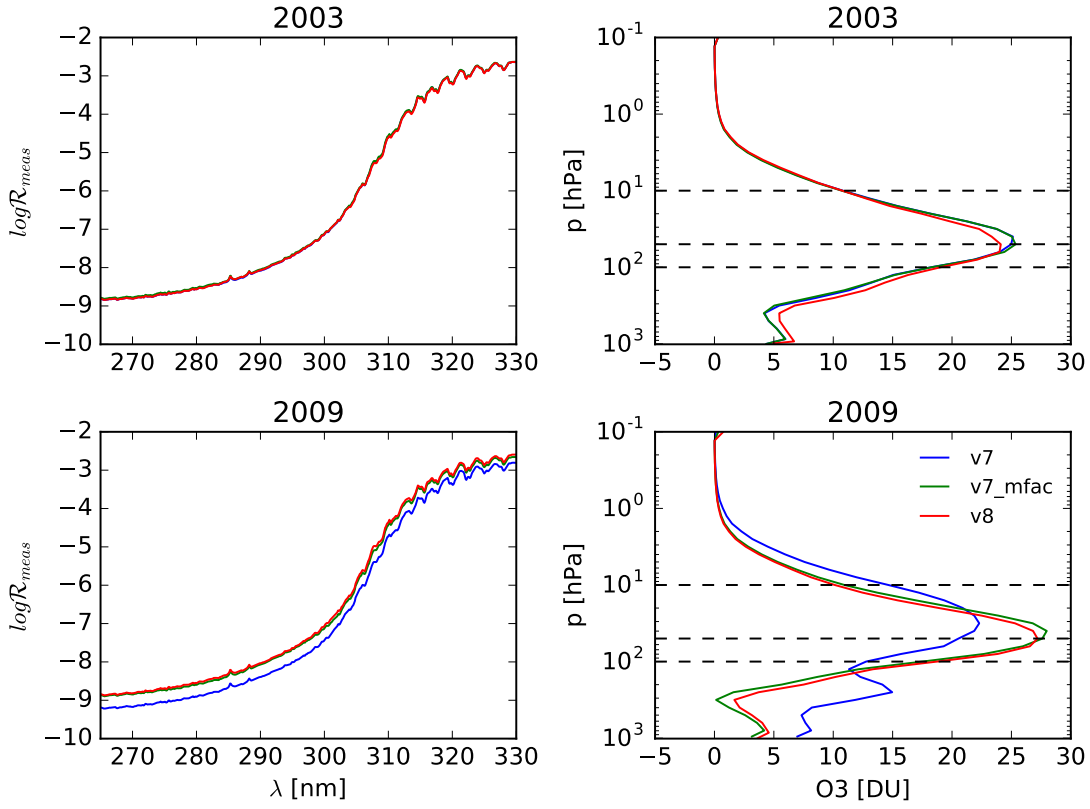

Figure 3. Top-left: Measured reflectance spectra for the year 2003. Note that the log scale is the natural logarithm, i.e. to the base e. The spectra are the medians for all states located close to the ozone sonde stations within the tropical latitude band 10°N - 10°S. Top-right: Corresponding retrieved ozone profiles (in Dobson Units per layer) with different colours representing various versions of L1 SCIAMACHY data used. The versions 7 with and without degradation correction almost overlap (blue and green lines) whereas version 8 with improved degradation correction has a visible difference in the ozone profile. Bottom-left and bottom-right figures hold for the year 2009. Note the remarkable difference between v7 and later versions with degradation corrections. Here the later two versions almost overlap compared to the case where no degradation is taken into account. The number of states in each data set with corresponding uncertainties is listed in Table 3. The dashed horizontal lines indicated the pressure levels 10, 50 and 100 hPa.

rived from them) vary from early to late in the SCIAMACHY mission. In Fig. 3 the results for 2003 are shown in the top panels and the results for 2009 are shown in the bottom panels. The left panels show the measured reflectance spectra used by the OPERA retrieval algorithm in estimating the ozone profile shown in the right panels. Each curve is a median of many ~~pixels~~nadir states, 347 for each dataset version of year 2003 and $\sim$ 400 for the year 2009. The spectrum and ozone profile of each nadir state is the average of all the retrieved pixels of the state, which are typically 64 pixels, sometimes less. The result in the figure is an average for all ~~the pixels~~ states over a narrow latitude band in the tropics from 10°N to 10°S. The different ~~colours of lines represent different~~ line colours represent different L1 datasets as labelled in the bottom right panel of the figure. The curves of ozone profiles in the top-right panel for 2003 representing v7 ~~,~~ and $\texttt{v7}_{\texttt{mfac}}$ ~~(blue and green respectively)~~ almost overlap each other showing minimal differences between the two versions and therefore the degradation corrections (m-factors) are also minimal. However, the curve representing v8 in red deviates from the other two visibly, which is hard to see in the reflectance spectra in the left panel. These differences are exacerbated for the year 2009 (later time of the mission) where the ozone profile of v7 is significantly different from $\texttt{v7}_{\texttt{mfac}}$ and v8 in its shape and amount of ozone. The corresponding measured spectra in the bottom-left-panel confirm these differences. We also observe visible differences between $\texttt{v7}_{\texttt{mfac}}$ and v8 indicating the intrinsic differences in the implementation of the degradation ~~corrections~~ correction between the two ~~dataset versions~~datasets. In the right panels of the figure are horizontal black-dashed lines demarcating the lower-middle stratosphere (100-10 hPa) with another line at 50 hPa. In dataset v7 there are large variations in the troposphere (1000-100 hPa) and a significant re-

duction of the peak of the ozone value in the stratosphere, suggesting the unreliability of this dataset for later years of the SCIAMACHY mission. The median errors and standard deviations (st. dev.) along with number of ~~pixels and convergence statistics for the retrievals in~~ states, number of iterations, and DFS statistics of the retrievals of Fig. 3 are listed in Table 3. The maximum number of iterations, `n_iter`, is set to 10 (see Table 2)~~, is set to 10 and~~ . The decreasing DFS value going from 2003 to 2009 is further illustrated in Fig. 4 which shows tropical DFS profiles for all months in 2003 and 2009. The DFS profiles for the earlier year (2003) are systematically higher than for the later year (2009). This means that the ~~median values of this quantity in the table conversions. This also suggests that further corrections to the L1 data are needed (See Sect. 7).~~

degradation leads to reduced information content.

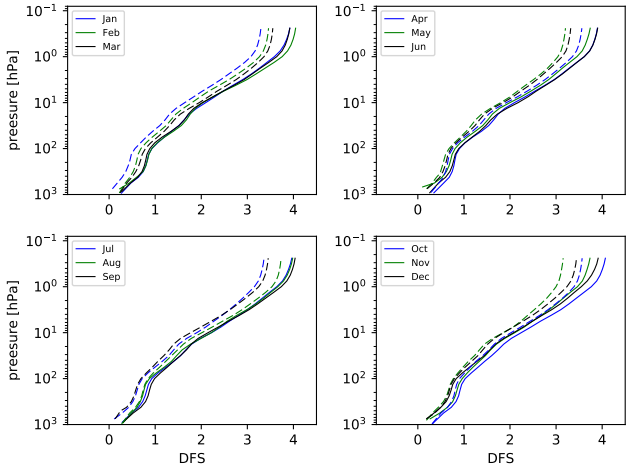

Figure 4. Degrees of freedom for signal (DFS) of SCIAMACHY ozone profile retrievals for individual months for nadir states in the tropics between 15°N - 15°S. The DFS profiles are shown for two years: 2003 in solid lines and 2009 in dashed lines. Here L1 `v8` is used.

4 Validation: Comparison with ozone sondes

Here we validate SCIAMACHY ozone profile retrievals with ozone sondes. We first compare the three different SCIAMACHY dataset versions as done above in Sect. 4.1, followed by validation results using `v8` dataset for all the years, 2003-2011. The aim is to analyse the quality of SCIAMACHY nadir ozone profile retrievals using `v7`, $\texttt{v7}_{\texttt{mfac}}$, and `v8` L1 data. With a UV-visible instrument it is very hard to retrieve an accurate ozone profile in the troposphere. This is clearly shown in Fig. 4, where the DFS in the troposphere, at pressure levels from $\sim 1000 - 100$ hPa, is at most 1. That means that there is at most one piece of information in the troposphere. Therefore, we focus the validation on the stratospheric part of the ozone profile between $\sim 100 - 10$ hPa. For validation, the retrieved ozone profiles are compared with balloon ozone sondes obtained from the World Ozone Ultraviolet Radiation Data Centre (WOUDC, 2011). The sonde is used if it is located within the four corners of the SCIAMACHY ~~pixel~~/state on the ground (which size is about $960\,\mathrm{km} \times 500\,\mathrm{km}$) and has a measurement date~~and~~ /time within 6 hours of the sonde.

The resulting geolocations of the selected sondes ~~from the WOUDC data set~~ are plotted in Fig. 5 for all years. The ~~validation algorithm implementing the collocation criteria is very similar to the one used by van Peet et al. (2014). For the methodology we refer to that paper. The~~ number of stations for the years 2003-2011 range from 38 to 66 with number of sondes ranging from 1 to 55 per station. ~~In comparing the retrieved profile with that of the sonde ,~~ The validation algorithm implementing the collocation criteria is similar to the one used by van Peet et al. (2014). We summarize it briefly here and refer to that paper for details.

An ozone sonde profile generally has a higher vertical resolution than a satellite retrieval, and can therefore observe more details in the ozone distribution. The validation should be done with the sonde profile as it would have been observed by the satellite, i.e. the sonde profile ~~is convolved with the averaging kernel (AK)~~ should be convolved according to the information present in the averaging kernel. The convolved (or smoothed) sonde profile is calculated by convolving the original sonde profile with the AK from the retrieval ~~characterizing the sensitivity of SCIAMACHY at each layer. This gives a~~ according to: $\boldsymbol{x}_{\mathbf{smooth}} = \boldsymbol{x}_a + \mathbf{A}\,(\boldsymbol{x}_{\mathrm{sonde}} - \boldsymbol{x}_a)$. The smoothed sonde profile ~~which is more suitable to compare with the profile retrieved from~~ is then compared to the ~~satellite instrument and~~ retrieved profiles from SCIAMACHY. Using a smoothed sonde profile instead of the original sonde profile to compare with the satellite retrieved profiles influences the results in Figs. 6-7~~which are~~ . This is discussed below. To get an impression of the shape ~~and effect of the~~ of the SCIAMACHY averaging kernels, we refer to ~~Appendix A. There in~~ Figure 2~~we show an example of SCIAMACHY averaging kernel shapes for a subset of the retrieved layers~~. In Figure 8 ~~we show the validation results for the case where the sondes were~~ a comparison between satellite and sonde profiles is shown for both cases: sonde profile convolved with the averaging kernel and ~~the case where the sondes were~~ not convolved. ~~Comparison of validation for three different dataset versions as labelled in the bottom right panel of the figure: dashed line is v7, dash-dotted line is $\texttt{v7}_{\texttt{mfac}}$ and solid line is v8. The validation is shown for Northern Hemisphere (NH), Tropics (Tr), and the Southern Hemisphere (SH) from top to bottom rows. For reference the uncertainty in the difference between the retrieved profile and the convolved sonde at each layer is shown for the v8 dataset.~~ The validation comparison is clearly better in the first case.

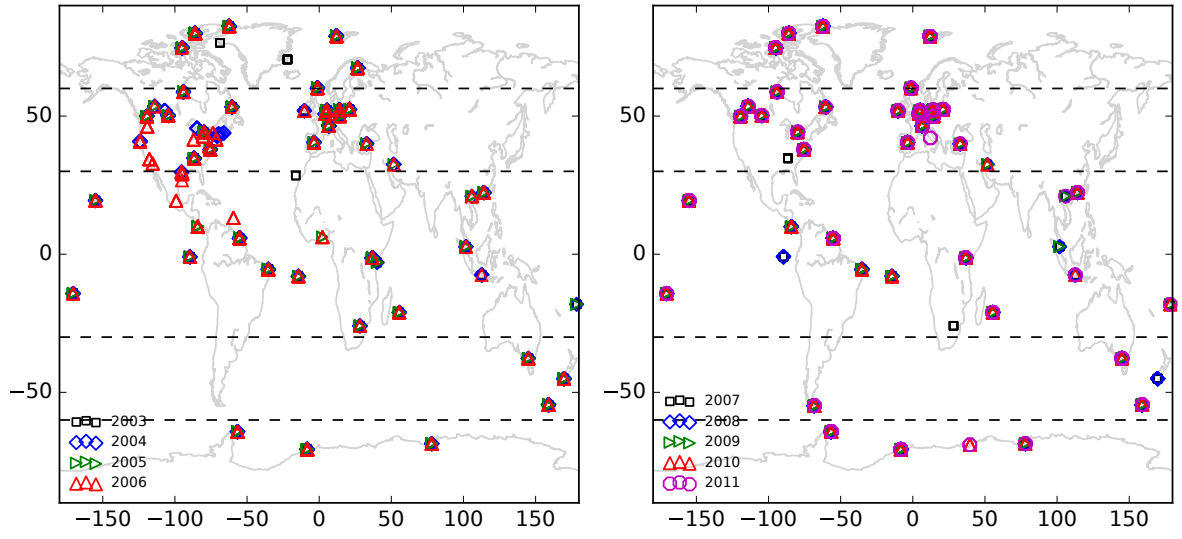

Figure 5. Collocated geolocations ~~indicating the location~~ of ~~the~~ satellite data and ozone ~~sondes~~ sonde stations used in the validation ~~for the dataset~~ of the L1 v8 dataset. Left: ~~collocated geolocations~~ Collocations for years 2003-2006 as labelled. Right: ~~the same~~ Same for years 2007-2011~~as labelled~~.

4.1 ~~Validation~~ Ozone profile validation comparison between versions v7, $v7_{mfac}$, and v8

In Fig. 6 ~~,~~ we show the ~~validation for the~~ ozone profile validation of the three data sets for the two years 2003 and ~~2009 and explicitly show the differences in the three datasets. The top row panels show the validation for the Southern Hemisphere (SH) with latitudes band~~ 2009. The results are given for five latitude bands: 90°~~S to~~ N to 60°N, 60°N to 30°~~S, middle row panels show the same for Tropics (Tr) with latitude band~~ N, 30°N to 30°S~~and finally bottom row panels show validation for the Northern Hemisphere (NH) with latitude band~~ , 30°~~N to~~ S to 60°S, and 60°S to 90°~~N. Different data sets: v7, $v7_{mfac}$ and v8 are shown in dashed, dash-dotted and solid lines, respectively, as labelled~~S. For reference the ~~errors~~ uncertainties (25%-75% percentiles) in the relative differences are shown only for v8 for all the latitude bands and both years as shaded regions. Each curve is the median difference between retrieved ozone ~~layer value~~ column per layer and the averaging-kernel smoothed ozone sonde value, normalized by the ozone sonde profiles. ~~The~~ In the lower-middle stratospheric region ~~is marked by yellow-dashed lines where better quality~~ a better agreement of the ~~nadir ozone data is expectedwith the sonde. An ideal agreement between sonde and satellite would give a difference of zero at all layer heights~~retrieval with the sonde is expected. Qualitatively, it seems that for most latitude regions ozone profiles retrieved from L1 v8 compare better with ozone sondes than profiles retrieved from the earlier L1 versions. For v8 profiles the comparison is generally better in 2003 than in 2009. The quantitative comparison results are given in the following.

~~Validation of ozone profiles retrieved using OPERA algorithm using SCIAMACHY L1 v8 dataset. Left column shows validation results for the years 2003-2006 and right column shows the same for years 2007-2011. Solid lines are median differences of retrieved profiles and, dashed lines are median differences with a priori profiles.~~

~~The relative percentage~~ The relative differences between the ~~nadir~~ retrieved profiles and the ~~sondes~~ sonde profiles are given in Table 4, where the top half of the table shows the results for the years 2003 and for datasets v7, $v7_{mfac}$ and v8~~for each zone: SH, Tr and NH. The same is listed in~~ , for three zones: Southern Hemisphere (SH): 90°S to 60°S, Tropics (Tr): 30°S to 30°N, and Northern Hemisphere (NH): 30°N to 90°N. In the bottom half of the table these quantities are given for the year 2009. From ~~the table~~ Table 4 we see that the ~~absolute values of the deviations (see third column, st. dev.~~ retrieved profile deviations (median differences in [%]) in the stratosphere are systematically smaller than in the troposphere~~(see fifth column)~~. These large spreads in ~~st. dev.~~ deviations of satellite retrievals from sondes are also visible in Fig. 6. Any deviation above $\sim 15\%$ in the stratosphere and above 20% in the troposphere are shown in bold ~~for reference~~ numbers for reference, as these are the required accuracy levels in the ESA ~~CCI programme~~ Ozone CCI project (http://www.esa-ozone-cci.org/). This behaviour is probably not only due to the relatively worsening sensitivity of ~~the nadir instrument to the tropospheric retrievals (van Peet et. al., *private communication*).~~ ~~Rather~~UV instruments in the troposphere. Rather, it might be due to the limited quality of

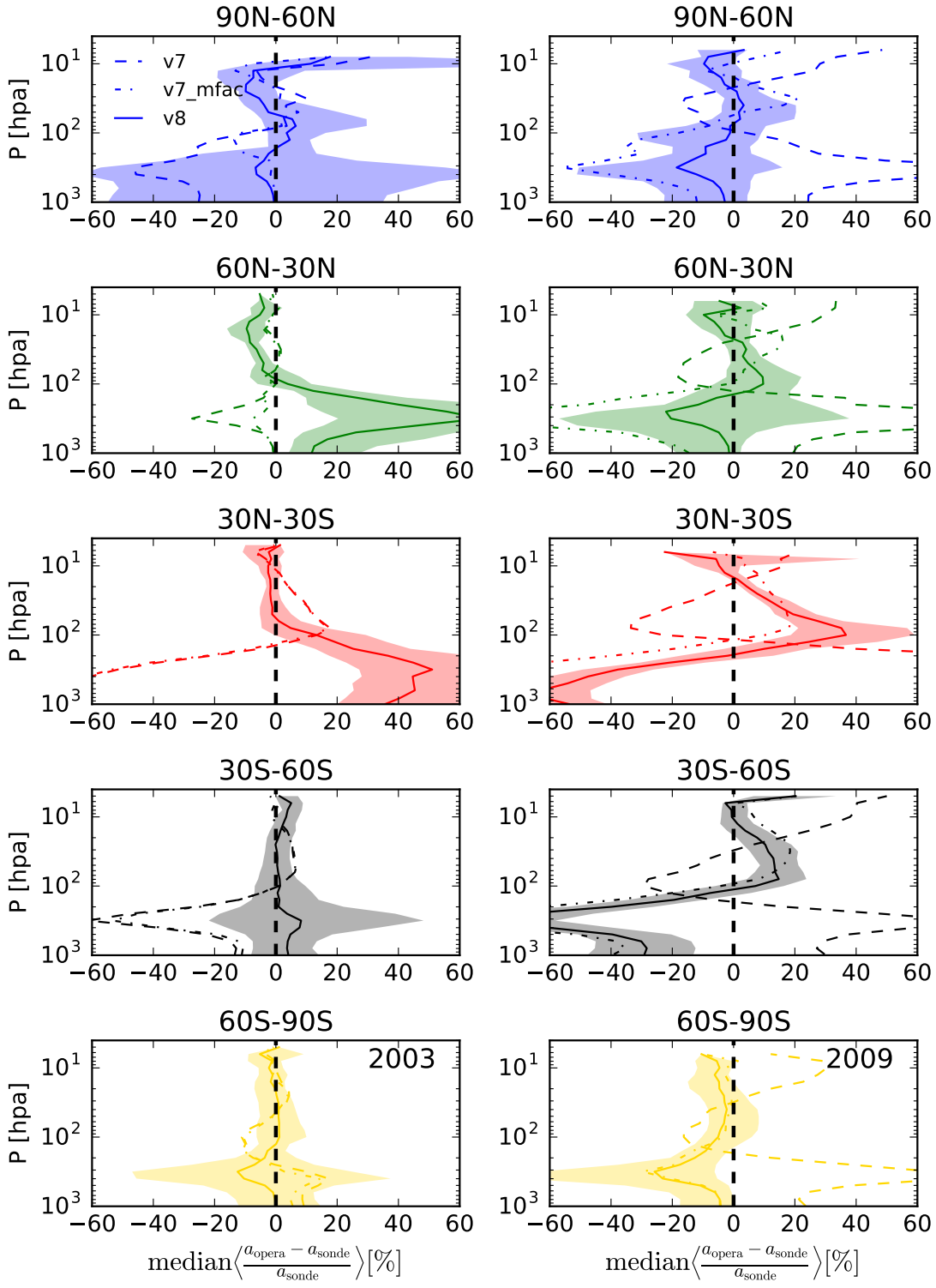

Figure 6. Relative difference between ozone profiles retrieved from three different SCIAMACHY L1 data versions and convolved ozone sonde profiles. The three L1 versions are indicated as: dashed line is v7, dash-dotted line is v7$_{\mathrm{mfac}}$ and solid line is v8. The shown quantity is the relative difference in ozone column per layer: (OPERA - sonde)/sonde. Results are shown in five rows for five latitude bands as indicated. The left column shows results for the year 2003, the right column for the year 2009. The uncertainty band (25-75 percentile difference) in the shaded area is shown for the v8 dataset.

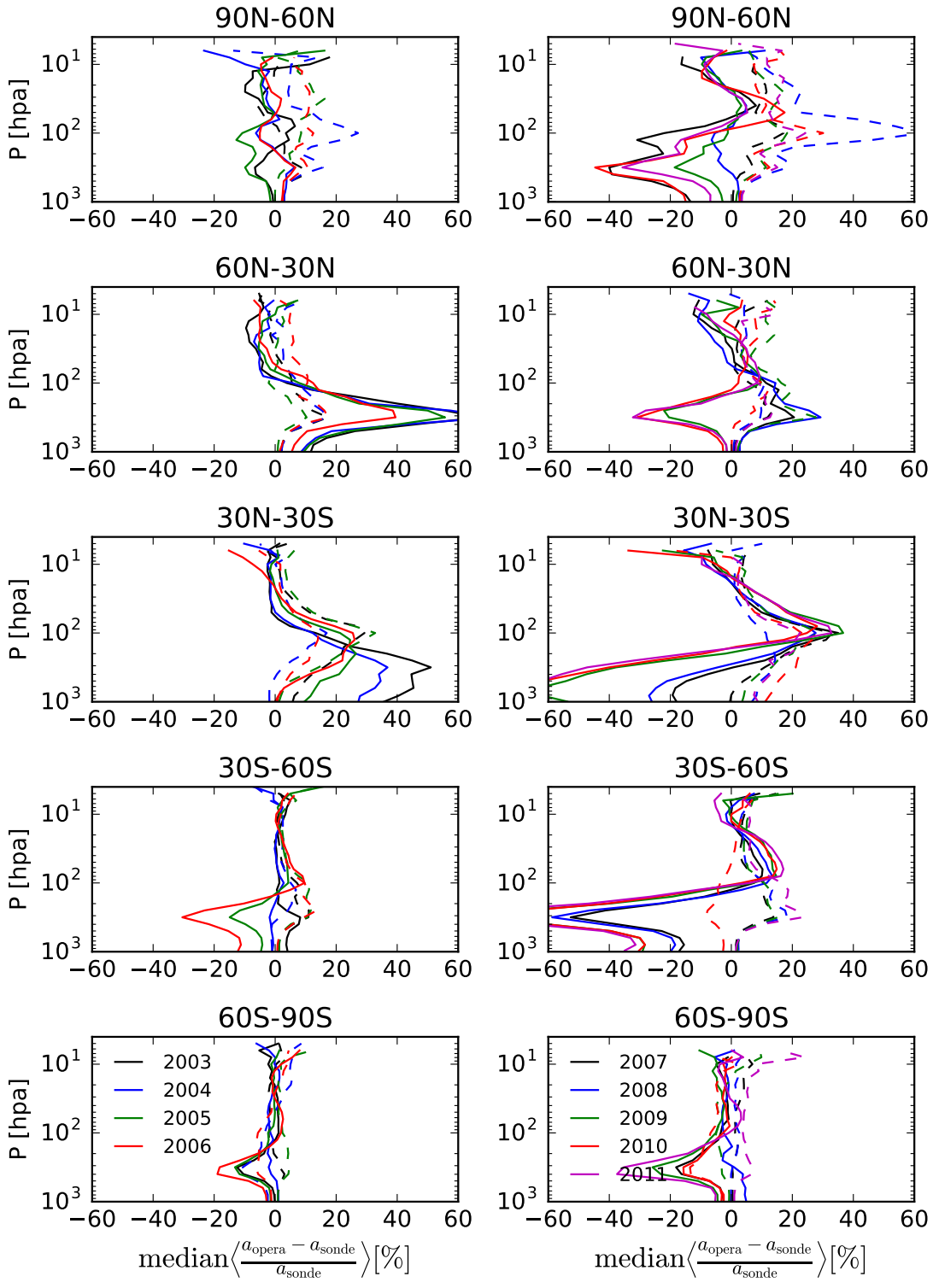

Figure 7. Relative difference between ozone profiles retrieved using SCIAMACHY L1 v8 data and convolved ozone sonde profiles, for the period 2003-2011. Results are shown for five latitude bands as indicated. Left column shows results for the years 2003-2006 and right column for the years 2007-2011. Solid lines are median differences of retrieved profiles and sonde profiles [(retrieval - sonde)/sonde], whereas dashed lines are median differences of a-priori profiles and sonde profiles [(a-priori - sonde)/sonde] in %.

the SCIAMACHY L1 data. Deviations in ~~validation~~ retrieved ozone profiles in the upper troposphere and lower stratosphere have been reported due to the ozone variability in a previous study of GOME-2 ~~nadir~~ data (Cai et al., 2012). However, in the stratosphere ~~(within the yellow dashed lines), the~~ the median deviations for 2003 are smaller for v8 for Tr and NH compared to the older dataset versions, whereas for the SH the three different datasets give comparable deviations. The deviations for 2009 in v8 in the stratosphere are smaller for SH and NH than in the older datasets; the deviations are comparable in the Tr zone between all datasets. Comparison of the ozone profile deviations between 2003 and 2009 show larger values for 2009, suggesting that the quality of L1 v8 data has degraded~~and is much worse than for earlier years (from comparison with 2003 v8 data)~~.

~~Validated level-2 product statistics Stratosphere 1000-100 Troposphere 100-10 Year # (SH, Tr, NH) dfs n_iter sza $\circ$ $\left\langle \frac{a_{\rm opera}-a_{\rm sonde}}{a_{\rm sonde}} \right\rangle$ [%] $\left\langle \frac{a_{\rm opera}-a_{\rm sonde}}{a_{\rm sonde}} \right\rangle$ [%] (SH, Tr, NH) (SH, Tr, NH) 2003 (32, 107, 260) 4.2 ± 0.4 5.0 ± 2.4 47.3 ± 16.3 (-5.0, -1.6, +0.8) (**+12.4, +40.4**, +2.5) 2004 (80, 121, 439) 4.3 ± 0.5 5.0 ± 2.1 50.6 ± 18.3 (-3.9, -1.3 , +0.1) (+5.9, **+27.8**, +0.1) 2005 (99, 121, 397) 4.3 ± 0.5 5.0 ± 2.2 58.2 ± 19.0 (-3.9, +1.3, +1.5) (+2.9, **+21.3**, -3.6) 2006 (78, 147, 481) 4.1 ± 0.5 5.0 ± 2.2 45.8 ± 18.9 (-1.4, +2.1, +2.8) (+5.3, **+17.4**, -9.7) 2007 (78, 88, 390) 4.1 ± 0.5 5.0 ± 2.5 59.9 ± 19.5 (+0.4, +4.2, +4.0) (-4.6, +0.7, -11.2) 2008 (119, 119, 373) 4.2 ± 0.5 5.0 ± 2.0 54.2 ± 19.5 (-0.3, +5.7, +6.4) (+3.9, -4.5, -12.0) 2009 (81, 101, 315) 3.8 ± 0.5 5.0 ± 2.4 54.1 ± 19.0 (+1.3, +11.6, +6.3) (-5.8, **-37.8, -22.9**) 2010 (90, 76, 360) 3.8 ± 0.5 5.0 ± 2.4 56.3 ± 19.1 (+3.0, +11.8, +6.5) (-12.1, **-40.1, -22.3**) 2011 (96, 60, 327) 3.8 ± 0.5 5.0 ± 2.5 58.8 ± 19.9 (+1.0, +11.6, +8.4) (-12.0, **-47.2, -22.8**)~~

4.2 Validation of v8 ozone profiles for ~~years~~ 2003-2011

In Fig. 7 we show validation results for the entire dataset ~~of~~ based on L1 v8 from the years 2003-2011~~organized according to latitude bands with top panels showing results for SH, middle panels for Tr and bottom panels for NH.~~, for the same five latitude zones as in Fig. 6. The left column ~~show results for (early)~~ shows results for the earlier years 2003-2006 and the right column for ~~(later)~~ the later years 2007-2011. The solid lines correspond to the difference between satellite and sonde (convolved with satellite AK) normalised by the sonde profile~~and~~ , whereas the dashed lines correspond to the difference ~~with the a priori~~ between satellite and a-priori profiles used in the retrieval (see Table 2). The number of collocated pixels for all the latitude bands for each year ~~is~~ are listed in Table 5 along with median ~~degrees-of-freedom (DFS, see Sect. 2.2),~~ DFS, median number of iterations required to achieve convergence, the median solar ~~azimuth~~ zenith angle and the median deviations in % for each zone in stratosphere and troposphere~~in the last two columns~~. From Fig. 7 we note that validation for all latitude bands show in general smaller deviations from the ~~centre (zero)~~ zero line for earlier years ~~(left column), and~~ than for later years~~(right column)~~ . For later years the agreement with sondes ~~become~~ becomes worse especially for tropics and NH ~~(right middle and bottom panels)~~bands. The median deviations ~~in the sixth and seventh columns of~~ given in Table 5 show often values higher than 20% (in boldface) for the troposphere whereas these values are less than 15% for the stratosphere deeming them within specifications according to ~~ESA~~ the Ozone CCI requirements (see Sect. ~~4.3~~4.1). It should be noted~~however ,~~ however, that the large deviations in ~~the tropospheric ozone 1000-100~~ tropospheric ozone are systematically higher ~~(~~than those for the ~~for stratosphere)~~ stratosphere for all zones and the years even for v8, ~~where~~ whereas such deviations are not observed for instance with GOME-2 nadir profiles ~~(van Peet et al. , *private communication*) .~~ (van Peet et al., 2014).

It can be seen from Fig. 7 that the vertical pattern of differences has changed significantly (and not just the absolute differences) over the instrument lifetime. This important to consider when applying the profiles for ozone layer studies.

This validation of ozone profiles based on L1 v8 suggests that the quality of nadir SCIAMACHY L1 data ~~is still poor and can~~ can still be improved upon. It affects the lowest troposphere in the beginning of the mission and gets worse due to instrument degradation. This is still uncorrected in the UV wavelength range. ~~Also observe~~ Please also note the higher deviations in the year 2003 in ~~SH and Tr (left upper and middle panels) compared to the rest of the~~ NH and Tr latitude zones in Fig. 7 as compared to other early years. This ~~unique behaviour of~~ is a unique behaviour for 2003~~is discussed in Sect. 7. ~~; the cause is not clear, but it is probably related to calibration or instrument changes in the early mission. Further improvements are needed (see Sect. 5).

~~Vertically integrated ozone columns (in DU) for the years 2003-2006 in left column for latitude bands 45°S:55°S (top row), 55°S:70°S (middle row), 70°S:90°S (bottom row). Each circle is the minimum value of daily retrieved quantity. The same is shown for years 2007-2011 in the right column. The time series are shown for months from 1 August - 1 Dec as labelled in x-axis where a is August, s is September, o is October, n is November and d is December. Each dot is a median of the total column amount for that day corresponding to the latitude bands and its size represents the number of pixels (states) used in computing the median.~~

~~Same as in Figure **??** using assimilated MSR v2 data (see text). Daily minimum ozone is plotted for latitude band 70°S:90°S~~

~~Nadir ozone vertical profile medians shown in Dobson Units per layer for years 2003-2006 in the left column for latitude bands 45°S:55°S (top row), 55°S:70°S (middle~~

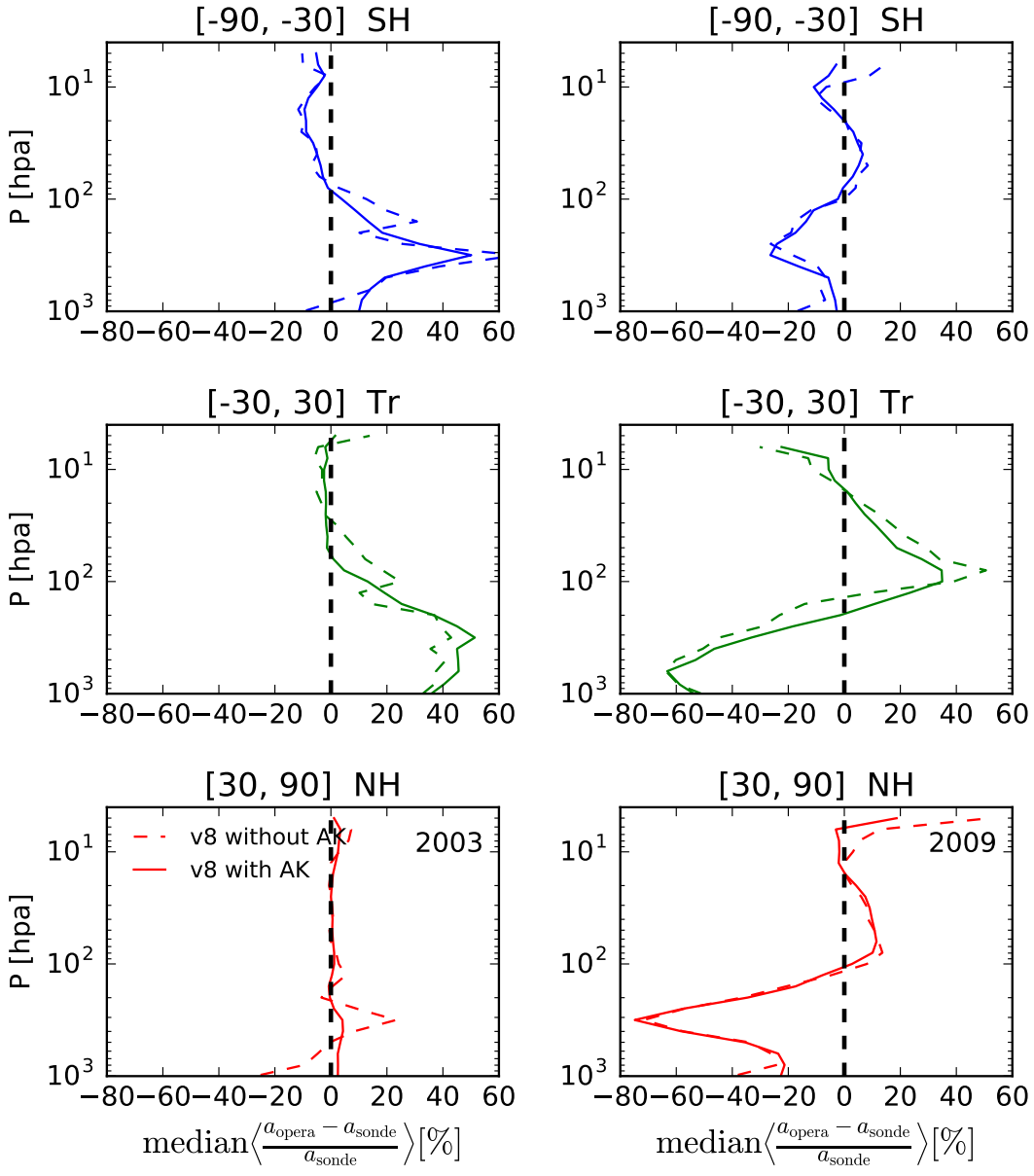

Figure 8. Comparison between SCIAMACHY retrieved ozone profiles and ozone sonde profiles with applying averaging kernels (AK, solid lines) and without applying averaging kernels (dashed lines). Here the L1 v8 data set is used.

~~row), 70°S:90° (bottom row). The same is shown for years 2007-2011 in the right column.~~

~~The deviations~~ The deviations found in SCIAMACHY v8 ~~validation results above for the stratosphere~~ ozone profiles can be compared~~for instance with GOME-2 validation results in van Peet et al. (2014)where they have used 16-layer pressure grid layer for retrievals~~, for instance, with GOME-2 ozone profile validation by van Peet et al. (2014). Their validation ~~in the troposphere also~~ of tropospheric ozone showed deviations ranging from a few percent to $\sim -30\%$ for the Northern Hemisphere, whereas we find ~~the deviations to~~ deviations that range from $\sim -10\%$ to -45%) for the year 2008 (blue line in right ~~panel~~ panels Fig. 7). In the Southern Hemisphere, however, we find ~~these~~ the deviations for year 2008 ~~(top right panel Fig. 7)~~ to range from a few percent to $\sim 20\%$, which is more comparable to the range of a few percent to $\sim -15\%$ ~~in~~ found by van Peet et al. (2014).

In Fig. 8, we show the effect on the validation of including the averaging kernel of the satellite retrievals to the ozone sonde profiles for the years 2003 (left panel) and 2009 (right panel). The validation results are clearly less noisy and smoother for the case where the AK was applied to the ozone sondes. For all validations presented in this section AK smoothing of ozone sonde profiles was used.

5 ~~SCIAMACHY results of the Antarctic Ozone Hole~~

~~In this section we show an application of the~~

5 Discussion of remaining L1 corrections

The accuracy of the retrieved ozone profile is primarily driven by the spectral and radiometric calibration of the measured L1 spectra. In this section we describe two potential L1 corrections that could further improve the quality of the SCIAMACHY L1 spectra: (1) retrieval of the instrumental slit function (SF) using solar spectra; (2) radiometric bias correction.

5.1 In-flight slit function calibration using solar measurements

One of the spectral calibrations often performed to assess the behaviour of an instrument in-flight is a fit of the instrumental slit function (also called instrumental spectral response function). The SF parameters of SCIAMACHY ~~dataset using~~ were measured pre-flight and are provided as key data in the L1 ~~v8 to infer the ozone in the Antarctic region. We apply the OPERA retrieval algorithm to all ground pixels south of 45° for the years 2003-2011 only for the months of (beginning of) August to (end of)November. The retrievals are separated in three latitude bands:~~ product. The slit function S of the instrument has different functional forms depending on the channel. For Channels 1-2 (relevant for our ozone profile retrieval) S is described by a single hyperbolic function:

$$\mathcal{S}(\lambda) = \frac{1}{a^2 + \lambda^2}. \quad (5)$$

The L1 key data provides the full width half maximum (FWHM), which is related to the a parameter in the equation above. This parameter can be solved in terms of the FWHM by using the fact that at the central point (λ_0) we have $S(\lambda_0) = 1/a^2$. Thus, $a = \frac{\mathrm{FWHM}}{2}^2$. At each given solar spectrum wavelength, λ_i, this functional shape is numerically computed between [~~45°S:55°S~~-1,~~55°S:70°S and 70°S:90°S shown in the top, middle and bottom rows of Fig. ?? respectively. The colour represents which year is labelled, showing early years (2003-2006) and later years (2007-2011) in the left and right columns of the figure, respectively. Each circle in the figure is the minimum value of the retrieved column for each day. The size of circle represents the number of pixels averaged per day and the range (minimum, maximum)of the number of pixels for all years and all latitude bands are listed in Table 5. The median uncertainties in the retrieved columns and their st. dev. are also listed in Table 5. The variations in the minimum integrated ozone are lowest for the latitude band: 45°S:55°S for all years (see top row of the figure) instead of a V-shaped dip appears in the southernmost latitude bands (see middle and bottom panels in the figure). This is as expected as the ozone depletion is stronger in the Antarctic region. Also the time of the minimum of the daily minimum integrated ozone columns occur between 15 September - 15 October which is also expected from other published results.~~

~~Antarctic Ozone nadir column statistics 45°S:55°S 55°S:70°S 70°S:90°S Year # 45°S:55°S # 55°S:70°S # 70°S:90°S $\langle\sigma_{O3}^{\mathrm{top}}\rangle$ $\langle\sigma_{O3}^{\mathrm{mid}}\rangle$ $\langle\sigma_{O3}^{\mathrm{bot}}\rangle$ 2003 2 305 512 922.68 ± 0.30 2.72 ± 0.48 2.74 ± 0.90 2004 4 2812 562 1012.74 ± 0.29 2.76 ± 0.27 2.65 ± 0.54 2005 4 2816 601106]2.78 ± 0.32 2.77 ± 0.32 2.72 ± 0.54 2006 2 304 601 853.00 ± 0.46 3.05 ± 0.35 3.23 ± 0.63 2007 1 303 603 602.67 ± 0.47 2.82 ± 0.42 2.87 ± 0.44 2008 2 254 451 683.05 ± 0.45 3.03 ± 0.37 3.05 ± 0.40 2009 2 291 601 1063.16 ± 0.56 3.04 ± 0.37 2.90 ± 0.61 2010 1 294 531 662.30 ± 0.64 3.26 ± 0.42 3.06 ± 0.42 2011 5 293 561 1103.14 ± 0.58 3.30 ± 0.39 3.30 ± 0.47~~

~~Statistics of SCIAMACHY nadir ozone profile retrievals for the Antarctic region. Year # Top # Mid # Bot Top Mid Bot $\langle\sigma_{O3}^{\mathrm{top}}\rangle$ $\langle\sigma_{O3}^{\mathrm{mid}}\rangle$ $\langle\sigma_{O3}^{\mathrm{bot}}\rangle$ 2003 1656 3514 3784 5 / 530.9 7.0/616.4 10.0/5750.2 0.55±0.82 0.59±1.07 0.44±1.182004 1777 4011 4845 5 / 556.6 6.0/616.5 10.0/660.1 0.56±0.83 0.62±1.07 0.46±1.182005 1877 3938 5103 5 / 579.2 6.0/647.7 10.0/713.5 0.56±0.84 0.62±1.07 0.46±1.222006 1727 3406 3278 5 / 559.2 6.0/652.8 10.0/1450.1 0.56±0.84 0.63±1.06 0.49±1.242007 1445 3141 2501 4 / 638.6 6.0/716.3 10.0/788.0 0.57±0.86 0.64±1.06 0.48±1.162008~~

1244 2629 2772 4 / 586.7 6.0/697.8 10.0/1672.0 0.57±0.84 0.63±1.09 0.48±1.232009 1664 3576 4019 4 / 645.2 6.0/753.0 10.0/1560.0 0.57±0.85 0.64±1.09 0.49±1.262010 1005 2071 2207 5 / 706.8 6.0/779.4 10.0/1826.8 0.56±0.86 0.65±1.11 0.49±1.272011 1776 3657 4481 4 / 757.6 6.0/786.0 10.0/3591.4 0.56±0.85 0.64±1.10 0.47±1.28

We compare these time series with the Multi Sensor Reanalysis of Ozone, version 2 (MSR v2)(**?**). The MSR uses data from TOMS, SBUV nm centred at λ_i. This shape can be manipulated with the following four parameters: additive constant (Offset O), multiplication factor (Gain G), GOME, displacement of the spectral peak (Shift D) and expansion and contraction of the spectral peak (Squeeze S). The high resolution solar reference spectrum from Dobber et al. (2008) is modified with these four parameters to best match the SCIAMACHY measured solar irradiance ($E(\lambda)$). First the spectral parameters, shift D and squeeze S, are applied to Eq. 5:

$$\mathcal{S}'_{\rm SD}(\lambda) = \mathcal{S}(\lambda[1 - S(\lambda)] + D(\lambda)), \quad (6)$$

followed by the radiometric parameters, gain G and offset O:

$$\mathcal{S}'_{\rm GOSD}(\lambda) = [\mathcal{S}'_{\rm SD}(\lambda)G(\lambda)] + O(\lambda). \quad (7)$$

The unit of D is nm whereas O, OMI, GOME-2 for latitudes south of 30°S resulting in a multi-decadal ozone column. The reprocessed ozone columns from all satellites are assimilated and bias corrected by calibrating with ozone columns obtained from Brewer and Dobson spectrophotometers in the WOUDC dataset. The SCIAMACHY L1 dataset included in the MSR v2 makes still use of v7 using the the total nadir ozone retrieval algorithm (TOSOMI) (**??**). The minimum ozone value available for any day from the MSR dataset is plotted for latitude band of 70°S:90°S in Fig. **??** and can be qualitatively compared to G and S are numeric factors. All four parameters depend on wavelength. The parameters FWHM and λ_0 at each wavelength, taken from the bottom two panels in Fig. **??**. The characteristic "V" shape in the Fig. **??** is in line with the minimum occurring between 15 September to 15 October for the years 2003-2011.The lowest value in the SCIAMACHY ozone in Fig **??** occurs between 1 September and 15 October for latitude bands of 55°S: 70°S and 70°S: 90°S in the middle and bottom panels. The ozone columns reach a plateau in Fig. **??** from 1 November for latitude band 55°S:70°S where as this feature is not visible for the band 70°S:90°S which is more consistent with the Fig. **??**. The overall level of the ozone column is at ∼ 150 in September for 70°S:90°S for the years 2004-2011 which is also qualitatively consistent with the MSR dataset.

It is useful to specifically compare the SCIAMACHY ozone total column in the stratosphere to the MSR v2 dataset for the year 2010, which was found to be an anomalous year in its behaviour of the ozone depletion (**?**). The Antarctic ozone hole had 40-60% less ozone destruction compared to the average of previous years (2005-2009). This is reflected in the right-panel of Fig. **??** where the minimum integrated ozone (in red) are above the rest of the years, showing higher levels of ozone from 1 August to 1 November with variations in the range of 250-150 DU. Comparing this with the right panel of Fig. **??** we note that SCIAMACHY nadir profile data does not pick up this anomalous behaviour of 2010 (also in red circles), the values in average are much lower than those in Fig. **??** and at most comparable to the rest of the years in Fig. **??** with variations in the range of 170 -100 DU. This could suggest that SCIAMACHY nadir profiles using plain L1 v8 data on its own may not be accurate enough (owing to remaining biases in L1 data, other instrumental issues like the instrumental coverage) to investigate inter-annual variability in Antarctic ozone depletion. Note that there is no SCIAMACHY data in early August south of latitude 70° due to the low Sun. Furthermore note that the MSR v2 does a time dependent bias correction before assimilation takes place. However, in the region of 55°S:70°S (mid-right panel of Fig. **??** we observe that the minimum ozone column for 2010 does exhibit the anomalous behaviour where it is higher compared to the rest of the years. This latitude region includes 70°S, which samples the vicinity of the outer edge of the ozone hole, this result does show that SCIAMACHY nadir profiles could be used to complement the inter-annual variability studies. The discrepancy between the minimum of the total ozone column in regions 55°S:70°S and 70°S:90°S can be further investigated by carrying out a bias study of the L1 data (see Sect. 7). key data, were identical for all the solar spectra throughout the mission. These values are given at certain wavelengths spread throughout Channels 1 and 2 and were interpolated for the wavelengths in-between. An Optimal Estimation (OE) algorithm was used to solve for the best parameter values fitting the solar spectrum measurements in-flight. The retrieved values of the four parameters at the solar spectrum wavelengths were then also applied to the Earth radiance spectra $I(\lambda)$ interpolated at the solar spectrum wavelengths.

In Fig. **??**, the ozone profiles are shown for various latitude bands as Thus for each wavelength of the solar spectrum the parameter values are computed using the above slit function model. Each spectral peak of the solar reference spectrum can be transformed by manipulating the SF using Offset, Gain, Shift, and Squeeze until it fits the measured spectrum. These spectral manipulations can be modelled as a polynomial of order n at the desired channels. The fit is checked by evaluating the relative difference between the solar irradiance measurement and simulation, which is the relative residual. The relative residuals for the best fit are shown in Fig. **??**. The median of the profiles for each latitude band and for each year is plotted as labelled with same colour coding as in Fig. **??**. In general the maximum of the ozone for all years decreases with the southernmost latitude bands

going from top to bottom of each column in Fig. **??**. The peak value of the ozone (maximum) decreases from ∼ 30 DU at latitude band of 45°S:55°S to ∼ 25 DU at the latitude band of 70°S:90°S for all the years. Furthermore, the curve tends to be bi-modal at the southernmost latitude band with a minimum value of ozone (a value of zero DU) at a pressure of 1009. Each curve is a residual for one solar spectrum, where the blue line is achieved by using only Gain and Offset in the model and the red line is achieved by including the Shift and Squeeze.

We find that the wavelength range 265-308 . This is the expected height of ozone depletion. The number of pixels for each year and for each latitude band are listed in Table 6 along with the median uncertainties in nm is the optimal range for obtaining the smallest residuals in Channel 1. However, the ozone profile retrieval algorithm requires spectra from 260 nm onwards. Because the part of Channel 1 above 308 nm is known to suffer of calibration problems, the SF fit in Channel 1 is performed for the range 260-308 nm. We ran the optimal estimation on all solar measurements of the ozone profile along with its spread. Columns 5-7 in Table 6 list the median number of iterations to reach conversion and the cost function that measures the deviation of simulated and measured spectraat n-th iteration. What can be seen is the increasing number of iterations and corresponding increase in SCIAMACHY mission for each day, which amounts to 3463 solar spectra. We convolved all spectra with {Offset, Gain, Shift, Squeeze} of polynomial order of = $\{2, 15, 2, -\}$ and found that the cost function (thus worsening retrievals) for the southernmost latitude bands.

6 Discussion

In the previous section the ozone hole in the Antarctic was analysed using SCIAMACHY data for years 2003-2011 using geolocations south of 45°. It is evident from Fig. **??** that the integrated ozone for the year 2003 (shown in black open circles)for the majority of cases reaches less than 1 (as expected) within 10 iterations in the Optimal Estimation routine. By using a spectral shift in the range 265-308 nm instead of in the left panels are outliers. The retrieved columns deviate significantly in the latitude band 55°S:70°S (middle row)in the month of August and the deviations are significant for the same year in latitude band 70°S:90°S (bottom row) for all the months. Furthermore, entire band 265-314 nm the residuals were significantly reduced (see left-panel in Fig. 9). No SF fit was possible between 308-314 nm. Thus, from 308 nm onwards we used the Channel 2 spectra.

The residuals in Channel 2 are somewhat larger than those in Channel 1 (see Fig. 9). The dashed lines in both panels of the total ozone columns of the year 2004 are similar to those of 2003 compared to the other years in the bottom row of Fig. **??**. This behaviour is reinstated further in Fig. **??**, in figure mark the ±2% residuals for reference. Dividing the relevant range of 308-330 nm into smaller ranges to get smaller residuals did not reduce the residuals any further. For the optimal wavelength divisions, we found the smallest residuals given by the polynomial orders of the left - middle and bottom rows where the ozone profiles in the those bands for years 2003 and 2004 show a significant deviation from the rest of the years. In fact, the southernmost ozone profiles also show that the deviations are strong for the years 2004, 2005. From the assimilated and calibrated MSR v2 dataset (**?**) shown in Fig. **??** there are no significant deviations of ozone columns for 2003 (left panel). In a study by (**?**), it was shown from the retrieval of Absorbing Aerosol Index (AAI) using SCIAMACHY nadir spectra from 340- 380set of {Offset, Gain, Shift, Squeeze} = $\{1, 4, 1, 2\}$. In Channel 2, we find that using spectral shift and squeeze in the range 308-330 nm that strong jumps in the neighbouring AAI were observed from day to day in the years 2003, 2004 and 2008. These are exactly correlated with the days where the instrument was heated up to get rid of the ice layer affecting the infrared wavelengths and their degradation. Probably this operation on SCIAMACHY instrument affects all the versions of reduces the relative residuals significantly. The relative errors of the L1 data. We suggest that these instrumental throughput changes are the cause of the deviating ozone profiles for the years 2003-2004solar irradiance in the wavelength range used for ozone profile retrieval, 265-330 nm, are only in the order of 10^{-5}. However, the relative residuals are in the order of a few percent. So we expect this error to propagate into the ozone profile retrieval. There are strong residuals at around 279 nm, 280 nm and 285 nm, due to the MgI and MgII lines in the solar spectra. These spectral windows were therefore not used in the ozone profile retrieval (see Sect. 2).

Figure 10 shows the temporal behaviour of the slit function parameters for Channel 1 (top row) and Channel 2 (bottom row) as density plots; the fitted parameter value for each wavelength and each day of the year is shown. The seasonal dependence of solar irradiance is observed, as expected, in the Gain parameter for both channels. The other parameters do not show a clear seasonal dependence or a clear trend over the mission time.

5.1 Radiometric bias correction

In Sect. 3, it was shown that As shown above, spectral corrections like shift and squeeze at the UV wavelengths can further improve the solar spectra by ∼ 4% several percent (see Fig. 9). However, the expected improvement from this is much less than the expected degradation and other remaining potential biases for the L1 data, which are increasing with the mission time. A preliminary analysis of this is shown in Fig. 11, where the mean ratio of observed to simulated reflectance spectra (R_{meas}/R_{sim}) is plotted for the day of June 24 for years 2003-2011in fading black

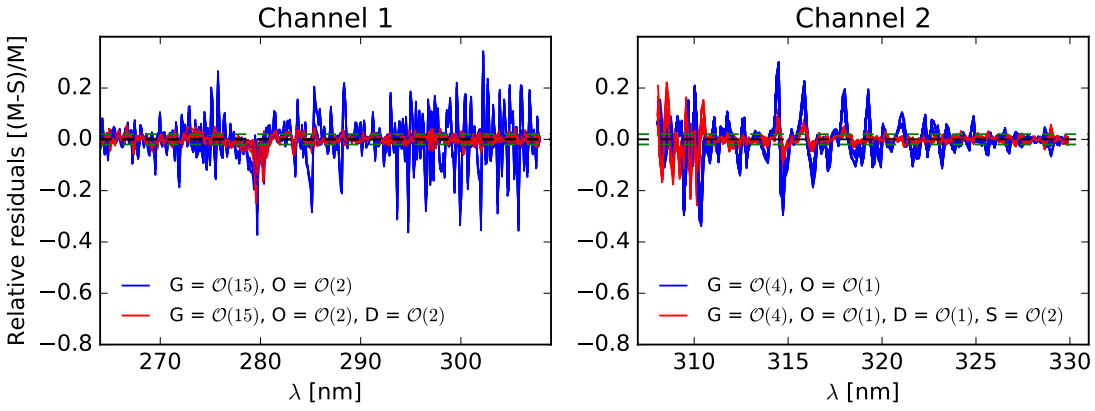

Figure 9. Relative residuals of daily SCIAMACHY L1 v8 solar spectra for Channel 1 (left) and Channel 2 (right), found by optimizing the slit function parameters O, G, D, S. The residual is defined as $(M\text{-}S)/M$, where M is the SCIAMACHY measured irradiance and S is the solar reference spectrum. For visibility, the residuals for only ~ 300 spectra are shown, which are representative of the entire mission from August 2002 to April 2012. The dashed lines mark the values of 0 and $\pm 2\%$.

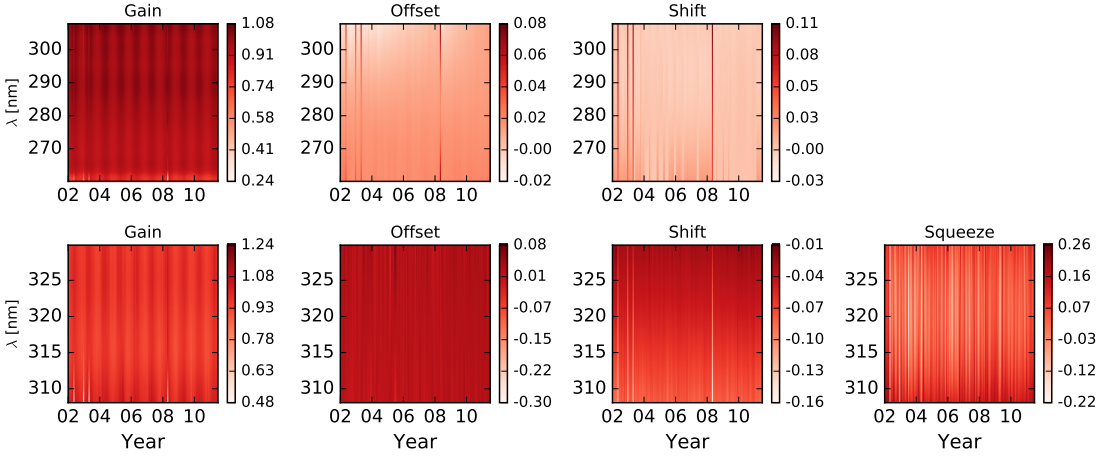

Figure 10. Temporal evolution of the slit function parameters for Channel 1 (top row) and Channel 2 (bottom row). The time series spans the entire mission for 3466 days, between 2002 and 2012. The ranges of the parameter values are shown to the right to each subplot.

~~to white colour~~. There is a strong deviation of this ratio ~~at 265-290~~from one below 300 nm and this becomes worse for later years~~, 2008-2011~~. A detailed study of this radiometric bias is beyond the scope of this paper. ~~However, a~~ Please note the odd behaviour of the reflectance ratio around 283 nm. This was found to be due to a jump in the value of the Earth radiance at the transition of cluster 3 to cluster 4 owing to the difference in integration time. This region is therefore blocked in our retrieval algorithm.

A L1 reflectance bias correction can significantly improve the quality of L1 data and will influence the validation and other results in this paper from their ozone retrievals. Furthermore applying these bias corrections would also make it meaningful to apply the spectral slit function corrections that can potentially improve the ozone retrievals further. Thus a detailed study of the effect of such bias corrections on the L1 data can be investigated against the quality of the ozone retrieval algorithm to better understand the quality of the SCIAMACHY nadir data.

6 Conclusions

We have performed SCIAMACHY nadir ozone profile ~~retrieval~~ retrievals using the OPERA algorithm ~~for~~ from three L1 data sets, namely v7, v7$_{\texttt{mfac}}$ and v8. We have used the latest complete ~~SCIAMACHY dataset (~~dataset v8 ~~)~~ for almost the entire SCIAMACHY mission length from 2003 to 2011. Differences between L1 datasets with and with-

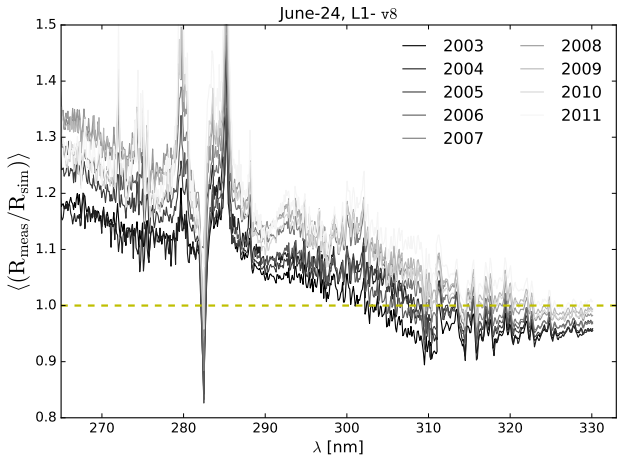

Figure 11. Mean ratio of observed (~~R_{meas}~~ R_{meas}) to simulated ~~model spectra~~ (~~R_{sim}~~ R_{sim}) reflectance spectra for ~~a~~ one day ~~of observations~~ for each year. The fading black colour goes from 2003 to 2011. A horizontal line where the ratio is one is shown for reference~~of the deviation of the ratio~~.~~Please note the odd behaviour of the spectral ratio around 283 which was found to be due to a jump in the spectral value of the Earth radiance between transitions of clusters 3 and 4 owing to the difference in the integration time between them. This region is blocked in our retrieval algorithm (See Sect. 2).~~

out degradation corrections (m-factors) were analysed in the wavelength range of 265-330 nm and show that the degradation correction including the scan-angle dependence in the ~~L1~~ v8 dataset gives the most smooth ozone profiles~~which~~ . This improved quality is also reflected in ~~their validation~~ the global validation of retrieved ozone profiles against ozone sondes. ~~Retrieving the instrument slit function in the UV range for this L1 data set also gives improvement of a few percent in the solar data through the mission length. However, the measured reflectance spectra show that the degradation in v8 is still significant because the ratio of the measured to simulated reflectance spectra (calculated from the radiative transfer model used in OPERA) can range from $\sim 1.1 - 1.4$ (see Fig. 11, Sect. 7). Furthermore the~~ The comparison between different L1 versions shows that v7 gives significantly worse ozone profiles, especially later in the mission ~~(2009)~~ compared to $v7_{mfac}$ and v8, where the profiles of v7 show a double peak for the year 2009 and an over-all reduced amount of ozone. Thus L1 v8 should be used for the nadir ozone profile applications of SCIAMACHY data.

~~Using all~~ We have found that further improvement of L1 ~~v8 data below 45°S for years 2003-2011 we investigated the Antarctic ozone profile behaviour in the austral spring season. The daily minimum of the total ozone column from August to end of November shows a characteristic "V" shaped curve with the dip in mid-September to beginning of October at the southernmost latitude bands. This is consistent with other satellite data sets (for example, (?)). The outliers are the years 2003-2004, which can also be seen in the profiles for various latitude bands averaged over the whole year. The overall peak value of ozone reduces with southernmost latitude bands and a prominent minimum in the ozone profile with vanishing ozone concentration appears at a height of 100~~data is possible. Retrieving the instrument slit function in the UV range for the v8 data set gives an improvement of a few percent in the solar data through the mission length. The measured reflectance spectra show that the degradation in v8 is still significant for some wavelengths, because the ratio of the measured to simulated reflectance spectra below 300 ~~, as expected.~~ nm can range from $\sim 1.1 - 1.4$. This could be corrected empirically by including a bias correction in the ozone profile retrievals.

7 ~~Averaging Kernels from OPERA retrievals using SCIAMACHY data~~

~~The averaging kernel (AK) of a retrieval represents the measurement sensitivity with respect to the true state of the atmosphere. The rows of the ozone profile averaging kernel matrix give the smoothing of the true profile as a function of the ozone retrieval layers. For an ideal retrieval, the curve of each row will peak at the nominal layer height with a spread that gives the vertical resolution of the retrieval. Example of the averaging kernel (AK) shape for a subset of seven layers from a 32-layer SCIAMACHY ozone profile retrieval. The triangles are the nominal altitudes of the retrieval layers. This subset of seven retrieval layers was selected uniformly ranging from top to bottom for clarity. From these AK curves it is clear that information on the ozone amount in a certain layer is also coming from other heights.~~

~~In Fig. 2 we show an example of the AK for an individual OPERA ozone profile retrieval for a pixel on 2004/01/07. In Fig. 8, we show the effect on the validation of including the satellite AK to the ozone sondes for the years 2003 (left panel) and 2009 (right panel). The validation results are clearly less noisy and smoother for the case where the AK was applied to the ozone sondes.~~

~~Comparison of validation of SCIAMACHY ozone profiles using ozone sondes with and without applying averaging kernels (AK) for the dataset v8. The solid lines indicate the use of the AK whereas the dashed lines indicate cases without AK. (cf. Fig. 6)~~

Acknowledgements. The authors would like to ~~acknowledge the SCIA-Visie project, funded by the Netherlands Space Office (NSO). The authors would also like to~~ thank Gijsbert Tilstra for support with SCIAMACHY data. The authors would also like to thank all data contributors to the World Ozone and Ultraviolet Radiation Data Centre (WOUDC) for submitting their data to a public database and Environment Canada for hosting the database. ESA and the SCIAMACHY Quality Working Group are acknowledged for providing and improving the SCIAMACHY L1 data. This work

was funded by the Netherlands Space Office (NSO) through the SCIA-Visie-Extensie project.

References

Bhartia, P. K., R. D. McPeters, C. L. Mateer, L. E. Flynn, and C. Wellemeyer: Algorithm for the estimation of vertical ozone profiles from the backscattered ultraviolet technique, J. Geophys. Res., 101(D13), 18793–18806, doi:10.1029/96JD01165, 1996.

Bhartia, P. K., McPeters, R. D., Flynn, L. E., Taylor, S., Kramarova, N. A., Frith, S., Fisher, B., and DeLand, M.: Solar Backscatter UV (SBUV) total ozone and profile algorithm, Atmos. Meas. Tech., 6, 2533-2548, https://doi.org/10.5194/amt-6-2533-2013, 2013.

Bovensmann, H., Burrows, M. J. P., Buchwitz, M., Frerick, J., Noel, S., Rozanov, V. V., Chance, K. V., and Goede, A. P. H.: SCIAMACHY: Mission objectives and measurement modes, J. Atmos. Sci., 56, pp. 127–150, 1999.

Bramstedt, K.: Scan-angle dependent degradation correction with the scanner model approach, Institute of Environmental Physics (IUP), Doc.No.: IUP-SCIA-TN-Mfactor, 2014.

Brinksma, E. J., Bracher, A., Lolkema, D. E., Segers, A. J., Boyd, I. S., Bramstedt, K., Claude, H., Godin-Beekmann, S., Hansen, G., Kopp, G., Leblanc, T., McDermid, I. S., Meijer, Y. J., Nakane, H., Parrish, A., von Savigny, C., Stebel, K., Swart, D. P. J., Taha, G., and Piters, A. J. M.: Geophysical validation of SCIAMACHY Limb Ozone Profiles, Atmos. Chem. Phys., 6, 197-209, https://doi.org/10.5194/acp-6-197-2006, 2006.

Burrows, J. P., Holzle, E., Goede, A. P. H., Visser, H., and Fricke, W.: SCIAMACHY – Scanning Imaging Absorption Spectrometer for Atmospheric Chartography, Acta Astronautica, 35, pp. 445–451, 1995.

Burrows, J. P., Weber, M., Buchwitz, M., Rozanov, V. V., Ladstätter-Weißenmayer, A., Richter, A., de Beek, R., Hoogen, R., Bramstedt, K., Eichmann, K.-U., Eisinger, M., and Perner, D.: The Global Ozone Monitoring Experiment (GOME): Mission concept and first scientific results, J. Atmos. Sci., 56, pp. 151–175, 1999.

Cai, Z., Y. Liu, X. Liu, K. Chance, C. R. Nowlan, R. Lang, R. Munro, and R. Suleiman: Characterization and correction of Global Ozone Monitoring Experiment 2 ultraviolet measurements and application to ozone profile retrievals, J. Geophys. Res., 117, D07305, doi:10.1029/2011JD017096, 2012.

Clerbaux, C., Boynard, A., Clarisse, L., George, M., Hadji-Lazaro, J., Herbin, H., Hurtmans, D., Pommier, M., Razavi, A., Turquety, S., Wespes, C., and Coheur, P.-F.: Monitoring of atmospheric composition using the thermal infrared IASI/MetOp sounder, Atmos. Chem. Phys., 9, 6041-6054, https://doi.org/10.5194/acp-9-6041-2009, 2009.

Deshler, T., Mercer, J. L., Smit, H. G. J., Stubi, R., Levrat, G., Johnson, B. J., Oltmans, S. J., Kivi, R., Thompson, A. M., Witte, J., Davies, J., Schmidlin, F. J., Brothers, G., and Sasaki, T.: Atmospheric comparison of electrochemical cell ozonesondes from different manufacturers, and with different cathode solution strengths: The Balloon Experiment on Standards for Ozonesondes, J. Geophys. Res., 113, doi: 10.1029/2007JD008975, 2008.

Dobber, M., Voors, R., Dirksen, R., Kleipool, Q., and Levelt, P.: The High-Resolution Solar Reference Spectrum between 250 and 550 nm and its Application to Measurements with the Ozone Monitoring Instrument, Solar Physics, 249, pp. 281–291, 2008.

Fortuin, J. P. F. and H. Kelder: An ozone climatology based on ozonesonde and satellite measurements, J. Geophys. Res., 103(D24), 31709–31734, doi:10.1029/1998JD200008, 1998.

Gottwald, M. and Bovensmann, H.: SCIAMACHY – Exploring the Changing Earth's Atmosphere, Springer, Dordrecht, the Netherlands, 2011.

Hubert, D., Lambert, J.-C., Verhoelst, T., Granville1, J., Keppens1, A., Baray, J.-L., Bourassa, A. E., Cortesi, U., Degenstein, D. A., Froidevaux, L., Godin-Beekmann, S., Hoppel, K. W., Johnson, B. J., Kyrölä, E., Leblanc1, T., Lichtenberg, G., Marchand, M., McElroy, C. T., Murtagh, D., Nakane, H., Portafaix, T., Querel, R., III, J. M. R., Salvador, J., Smit, H. G. J., Stebel, K., Steinbrecht, W., Strawbridge, K. B., Stübi, R., Swart, D. P. J., Taha, G., Tarasick, D. W., Thompson, A. M., Urban, J., van Gijsel, J. A. E., Malderen, R. V., von der Gathen, P., Walker, K. A., Wolfram, E., , and Zawodny, J. M.: Ground-based assessment of the bias and long-term stability of 14 limb and occultation ozone profile data records, Atmos. Meas. Tech., 9, pp. 2497-2534, https://doi.org/10.5194/amt-9-2497-2016, 2016.

Keppens, A., Lambert, J.-C., Granville, J., Miles, G., Siddans, R., van Peet, J. C. A., van der A, R. J., Hubert, D., Verhoelst, T., Delcloo, A., Godin-Beekmann, S., Kivi, R., Stübi, R., and Zehner, C.: Round-robin evaluation of nadir ozone profile retrievals: methodology and application to MetOp-A GOME-2, Atmos. Meas. Tech., 8, 2093-2120, https://doi.org/10.5194/amt-8-2093-2015, 2015.

Koelemeijer, R. B. A., J. F. de Haan, and P. Stammes: A database of spectral surface reflectivity in the range 335–772 nm derived from 5.5 years of GOME observations, J. Geophys. Res., 108, 4070, doi:10.1029/2002JD002429, D2, 2003.

Kroon, M., de Haan, J. F., Veefkind, J. P., Froidevaux, L., Wang, R., Kivi, R., and Hakkarainen, J. J.: Validation of operational ozone profiles from the Ozone Monitoring Instrument, J. Geophys. Res., 116, D18305, doi:10.1029/2010JD015100, 2011.

Levelt, P. F., Hilsenrath, E., Leppelmeier, G. W., van den Oord, G. B. J., Bhartia, P. K., Tamminen, J., de Haan, J. F., and Veefkind, J.: Science objectives of the Ozone Monitoring Instrument, IEEE Trans. Geosci. Remote Sens., 44, pp. 1199–1208, 2006.

Lichtenberg, G., Kleipool, Q., Krijger, J. M., van Soest, G., van Hees, R., Tilstra, L. G., Acarreta, J. R., Aben, I., Ahlers, B., Bovensmann, H., Chance, K., Gloudemans, A. M. S., Hoogeveen, R. W. M., Jongma, R. T. N., Noël, S., Piters, A., Schrijver, H., Schrijvers, C., Sioris, C. E., Skupin, J., Slijkhuis, S., Stammes, P., and Wuttke, M.: SCIAMACHY Level 1 data: calibration concept and in-flight calibration, Atmos. Chem. Phys., 6, 5347-5367, https://doi.org/10.5194/acp-6-5347-2006, 2006.

Liu, X., Bhartia, P. K., Chance, K., Spurr, R. J. D., and Kurosu, T. P.: Ozone profile retrievals from the Ozone Monitoring Instrument, Atmos. Chem. Phys., 10, 2521-2537, https://doi.org/10.5194/acp-10-2521-2010, 2010.

Malicet, J., Daumont, D., Charbonnier, J., Parisse, C., Chakir, A., and Brion, J.: Ozone UV spectroscopy. II – Absorption cross-sections and temperature dependence, J. Atmos. Chem., 21, pp. 263–273, 1995.

McPeters, R. D., G. J. Labow, and J. A. Logan: Ozone climatological profiles for satellite retrieval algorithms, J. Geophys. Res., 112, D05308, doi:10.1029/2005JD006823, 2007.

Mieruch, S., Weber, M., von Savigny, C., Rozanov, A., Bovensmann, H., Burrows, J. P., Bernath, P. F., Boone, C. D., Froidevaux, L., Gordley, L. L., Mlynczak, M. G., Russell III, J. M., Thomason, L. W., Walker, K. A., and Zawodny, J. M.: Global and long-term comparison of SCIAMACHY limb ozone profiles with correlative satellite data (2002–2008), Atmos. Meas. Tech., 5, 771-788, https://doi.org/10.5194/amt-5-771-2012, 2012.

Mijling, B., Tuinder, O. N. E., van Oss, R. F., and van der A, R. J.: Improving ozone profile retrieval from spaceborne UV backscatter spectrometers using convergence behaviour diagnostics, Atmos. Meas. Tech., 3, 1555-1568, https://doi.org/10.5194/amt-3-1555-2010, 2010.

Miles, G. M., Siddans, R., Kerridge, B. J., Latter, B. G., and Richards, N. A. D.: Tropospheric ozone and ozone profiles retrieved from GOME-2 and their validation, Atmos. Meas. Tech., 8, 385-398, https://doi.org/10.5194/amt-8-385-2015, 2015.

Munro, R., Lang, R., Klaes, D., Poli, G., Retscher, C., Lindstrot, R., Huckle, R., Lacan, A., Grzegorski, M., Holdak, A., Kokhanovsky, A., Livschitz, J., and Eisinger, M.: The GOME-2 instrument on the Metop series of satellites: instrument design, calibration, and level 1 data processing – an overview, Atmos. Meas. Tech., 9, 1279-1301, https://doi.org/10.5194/amt-9-1279-2016, 2016.

Rodgers, C. D.: Inverse Methods for Atmospheric Sounding, World Scientific Publishing, 2000.

Slijkhuis, S., Stammes, P., Levelt, P. F., and de Vries, J.: Envisat-1 SCIAMACHY Level 0 to 1c Processing Algorithm Theoretical Basis Document, ENV-ATB-DLR-SCIA- 0041, Deutsches Zentrum fuer Luft- und Raumfahrt e.V., Oberpfaffenhofen, Germany, 2001.

Smit, H. G. J., Straeter, W., Johnson, B. J., Oltmans, S. J., Davies, J., Tarasick, D. W., Hoegger, B., Stubi, R., Schmidlin, F. J., Northam, T., Thompson, A. M., Witte, J. C., Boyd, I., and Posny, F.: Assessment of the performance of ECC-ozonesondes under quasi-flight conditions in the environmental simulation chamber: Insights from the Juelich Ozone Sonde Intercomparison Experiment (JOSIE), J. Geophys. Res., 112, 19306, 2007.

Staehelin, J.: Global atmospheric ozone monitoring, WMO Bulletin, 57 (1), pp. 45–54, January 2008.

Tuinder, O. N. E., van Oss, R., Mijling, B., and Tilstra, L. G.: OPERA Software User Manual, KNMI-SUM-Manual-2014-01, 2014.

van der A, R. J., R. F. van Oss, A. J. M. Piters, J. P. F. Fortuin, Y. J. Meijer, and H. M. Kelder, Ozone profile retrieval from recalibrated Global Ozone Monitoring Experiment data, J. Geophys. Res., 107(D15), doi:10.1029/2001JD000696, 2002.

van Oss, R. F. and Spurr, R.: Fast and accurate 4 and 6 stream linearised discrete ordinate radiative transfer models for ozone profile remote sensing retrieval, J. Quant. Spectrosc. Radiat. Transfer, 75, pp. 177–220, 2002.

van Peet, J. C. A., van der A, R. J., Tuinder, O. N. E., Wolfram, E., Salvador, J., Levelt, P. F., and Kelder, H. M.: Ozone ProfilE Retrieval Algorithm (OPERA) for nadir-looking satellite instruments in the UV–VIS, Atmos. Meas. Tech., 7, 859-876, https://doi.org/10.5194/amt-7-859-2014, 2014.

Wang, P., Stammes, P., van der A, R., Pinardi, G., and van Roozendael, M.: FRESCO+: an improved O2 A-band cloud retrieval algorithm for tropospheric trace gas retrievals, Atmos. Chem. Phys., 8, 6565-6576, https://doi.org/10.5194/acp-8-6565-2008, 2008.

Worden, H. M., et al., Comparisons of Tropospheric Emission Spectrometer (TES) ozone profiles to ozonesondes: Methods and initial results, J. Geophys. Res., 112, D03309, doi:10.1029/2006JD007258, 2007.

Table 2. Parameter settings in the OPERA algorithm for ~~the~~ SCIAMACHY nadir O_3 profile retrieval

Physical parameter ~~/physics~~ or process	Description	Setting used in OPERA
~~Model~~ Forward radiative transfer model	LIDORT-A	van Oss and Spurr (2002)
	number of streams ~~: LIDORT-A~~	6
Raman scattering	on~~or off~~ /off option in LIDORT-A	off
O_3 absorption ~~cross-sections~~ cross-section	~~temperature parametrised~~ temperature-parametrised database using five temperatures ~~for the polynomial temperature parametrised expansion~~	~~Malicet et al. (1995, e.g.)~~Malicet et al. (1995)
~~Brion, Daumont and Malicet cross-section~~		
~~Climatology~~ O_3 profile climatology	a-priori O3 ~~a priori profile has three different ozone~~ profile climatologies	~~?Fortuin and Kelder (1998); McPeters et al. (2007)~~ McPe
Temperature	temperature profile ~~: ECMWF~~	ECMWF re-analysis
Noise floor	~~systematic~~ relative error of measured reflectance	0.015 (for all datasets)
Retrieval method	Optimal estimation	Rodgers (2000); van der A et al. (2002)
Wavelength window	variable bands	~~(can be set independent of instrument channels)~~ 265 - 330 nm
	blocked MgI, MgII lines	284.5 - 286.5 nm, 278.0 - 280.5 nm
Maximum number of ~~Iteration~~ iterations	convergence based on decrease of the relative cost function	10
Pressure grid	number of layers ~~heights~~ for retrieval	~~32~~ 31
	pressure levels	1000.0, 749.89, 583.48, 421.7, 316.23, 237.14, 177.83, 133.35, 100.0, 74.99, 56.23, 42.17, 31.63, 23.71, 17.78, 13.33, 10.0, 7.5, 5.62, 4.22, 3.16, 2.37, 1.78, 1.33, 1.0, 0.75, 0.56, 0.42, 0.32, 0.24, 0.18, 0.13 hPa
Fit parameters	ozone column per layer	
	~~Fit albedo~~ surface albedo or cloud albedo	~~for~~ if cloud fraction < 0.20, ~~fit for surface albedoelse fit for~~ surface albedo; else cloud albedo
Cloud model	~~parameters:~~ effective cloud fraction ~~height, pressure profiles~~ and cloud height	FRESCO+ (Wang et al., 2008)
~~surface albedo Koelemeijer et al. (2003)~~		

Table 3. ~~Median~~ Statistics of the uncertainties of the L2 ozone profile products that are retrieved using three different versions of L1 datasets (described in Sect. 2.1). This table corresponds to the ~~level-2 product~~ statistics of the curves shown in Fig. 3.

Year	~~version~~ level-1 version	# ~~Pixels~~ states	~~n_iter~~ number of iterations	DFS	$\langle \sigma^{R_{\rm meas}}/R_{\rm meas} \rangle$	std($\langle \sigma^{R_{\rm meas}}/R_{\rm meas} \rangle$)	$\langle \sigma_{O3}/O3 \rangle$	std(
2003	v7	347	5.0±2.3	5.5±0.6	0.015	0.060	0.072	
2003	$\texttt{v7}_{\texttt{mfac}}$	347	5.0±2.3	5.5±0.6	0.015	0.059	0.075	
2003	v8	347	5.0±2.0	5.5±0.6	0.015	0.013	0.072	
2009	v7	392	6.0±1.9	4.9±0.4	0.052	0.239	0.056	
2009	$\texttt{v7}_{\texttt{mfac}}$	408	7.0±2.2	4.9±0.5	0.051	0.239	0.076	
2009	v8	409	5.0±2.2	4.9±0.4	0.054	0.260	0.082	

Column 1: L1 data year, *Column 2*: Dataset version, *Column 3*: Number of states used, *Column 4*: Median number of iterations ± standard deviation, *Column 5*: Median degrees-of-freedom ± stan
Column 6: Median relative uncertainty of converged reflectance spectra in the wavelength band used, *Column 7*: Standard deviation of quantity in *Column 6*, *Column 8*: Relative uncertainty in retrie
Column 9: Standard deviation of quantity in *Column 8*.

Table 4. ~~Validation statistics~~ Statistics of ~~various dataset~~ relative differences between retrieved ozone profiles and ozone sondes for 2003 and 2009, per latitude zone, for the three L1 data versions. All numbers in %. Bold numbers are exceeding ESA CCI accuracy thresholds.

	Stratosphere [~~1000-100~~100-10] hPa	~~st. dev.~~	Troposphere [~~100-10~~1000-100] hPa	~~st. dev.~~
~~Zone~~ Latitude	Range [%]	~~Range~~ Median	Range [%]	Median
~~2003~~ 2003	v7			
SH	[-6.2 2.1]	-1.0	[**-38.4** -6.2]	~~**-12.7**~~ -12.7
Tr	[-1.6 **17.7**]	+8.3	[**-71.9** 13.5]	**-51.6**
NH	[-2.5 5.2]	+2.9	[**-39.8** -2.5]	-11.2
	$v7_{mfac}$			
SH	[-6.5 1.3]	-1.4	[-8.9 -0.3]	-3.8
Tr	[-1.3 **17.0**]	+8.9	[**-72.2** 12.6]	**-53.6**
NH	[-2.4 4.7]	+2.7	[**-35.2** -2.4]	-11.1
	v8			
SH	[-9.4 3.9]	-5.0	[3.9 **43.1**]	~~**+12.4**~~ +12.4
Tr	[-2.5 ~~**13.2**~~13.2]	-1.6	[13.2 **51.0**]	**+40.4**
NH	[0.0 2.4]	+0.8	[-0.5 4.0]	+2.5
~~2009~~ 2009	v7			
SH	[**-16.4** **28.9**]	-4.7	[-1.7 **100.7**]	**28.1**
Tr	[**-33.5** **16.8**]	~~**-13.3**~~ -13.3	[**-23.1** **220.0**]	**179.1**
NH	[**-25.5** **35.8**]	-0.9	[**-25.5** **72.5**]	**26.1**
	$v7_{mfac}$			
SH	[-8.8 **15.2**]	+2.2	[**-66.9** -8.8]	**-29.8**
Tr	[3.6 **18.5**]	~~**+12.3**~~ +12.3	[**-109.0** 10.3]	**-84.7**
NH	[-4.1 14.1]	+8.4	[**-99.4** -4.1]	**-30.6**
	v8			
SH	[-9.7 4.0]	+1.3	[**-19.2** 0.4]	-5.8
Tr	[-4.7 **36.7**]	~~**+11.6**~~ +11.6	[**-63.0** **36.7**]	**-37.8**
NH	[-2.1 10.7]	+6.3	[**-71.8** 2.4]	**-22.9**

Column 1: Year followed by latitude zone, *Column 2*: [Minimum Maximum] of relative differences $\left\langle \frac{a_{\mathrm{opera}} - a_{\mathrm{sonde}}}{a_{\mathrm{sonde}}} \right\rangle$ [%] in the stratosphere, *Column 3*: Median of relative differences for the stratosphere over the specified altitude range and latitude zone, *Column 4,5*: Same as *Column 2,3* but for the troposphere.

Table 5. Validation statistics of retrieved ozone profiles from L1 v8 for the period 2003-2011. Bold numbers in the medians of relative differences are exceeding ESA CCI accuracy thresholds.

					Stratosphere [100-10] hPa	Troposphere [1000-100] hPa
Year	# (SH, Tr, NH)	DFS	n_iter	SZA [°]	$\left\langle \frac{a_{\mathrm{opera}}-a_{\mathrm{sonde}}}{a_{\mathrm{sonde}}} \right\rangle$ [%] (SH, Tr, NH)	$\left\langle \frac{a_{\mathrm{opera}}-a_{\mathrm{sonde}}}{a_{\mathrm{sonde}}} \right\rangle$ [%] (SH, Tr, NH)
2003	(32, 107, 260)	4.2 ± 0.4	5.0 ± 2.4	47.3 ± 16.3	(-5.0, -1.6, +0.8)	(+12.4, **+40.4**, +2.5)
2004	(80, 121, 439)	4.3 ± 0.5	5.0 ± 2.1	50.6 ± 18.3	(-3.9, -1.3 , +0.1)	(+5.9, **+27.8**, +0.1)
2005	(99, 121, 397)	4.3 ± 0.5	5.0 ± 2.2	58.2 ± 19.0	(-3.9, +1.3, +1.5)	(+2.9, **+21.3**, -3.6)
2006	(78, 147, 481)	4.1 ± 0.5	5.0 ± 2.2	45.8 ± 18.9	(-1.4, +2.1, +2.8)	(+5.3, **+17.4**, -9.7)
2007	(78, 88, 390)	4.1 ± 0.5	5.0 ± 2.5	59.9 ± 19.5	(+0.4, +4.2, +4.0)	(-4.6, +0.7, -11.2)
2008	(119, 119, 373)	4.2 ± 0.5	5.0 ± 2.0	54.2 ± 19.5	(-0.3, +5.7, +6.4)	(+3.9, -4.5, -12.0)
2009	(81, 101, 315)	3.8 ± 0.5	5.0 ± 2.4	54.1 ± 19.0	(+1.3, +11.6, +6.3)	(-5.8, **-37.8**, **-22.9**)
2010	(90, 76, 360)	3.8 ± 0.5	5.0 ± 2.4	56.3 ± 19.1	(+3.0, +11.8, +6.5)	(-12.1, **-40.1**, **-22.3**)
2011	(96, 60, 327)	3.8 ± 0.5	5.0 ± 2.5	58.8 ± 19.9	(+1.0, +11.6, +8.4)	(-12.0, **-47.2**, **-22.8**)

Column 1: Year, *Column 2*: Number of states per latitude zone: Southern Hemisphere (SH), Tropics (Tr), Northern Hemisphere (NH), *Column 3*: Median DFS, *Column 4*: Median number of iterations, *Column 5*: Median solar zenith angle $\pm$ standard deviation for all states in that row, *Column 6*: Medians of relative difference between retrieved and sonde profiles for stratosphere for SH, Tr and NH over the specified altitude range and for the corresponding latitude band, *Column 7*: Same as in *Column 6* for troposphere.